Long-lasting memory of jasmonic acid-dependent immunity requires DNA demethylation and ARGONAUTE1

Samuel Wilkinson
University of Sheffield https://orcid.org/0000-0002-4908-8766
Amos Muench
University of Sheffield
Robert Wilson
University of Sheffield https://orcid.org/0000-0001-9010-1363
Kourosh Hooshmand
Aarhus University
Michael Henderson
University of Sheffield
Emma Moffat
University of Sheffield https://orcid.org/0000-0002-8559-2142
Joost Stassen
University of Sheffield https://orcid.org/0000-0001-5483-325X
Ana López Sánchez
University of Sheffield
Inge Fomsgaard
Aarhus University
Paal Krokene
Norwegian Institute for Bioeconomy Research
Melissa Magerøy
Norwegian Institute for Bioeconomy Research
Jurriaan Ton (✉ j.ton@sheffield.ac.uk)
University of Sheffield https://orcid.org/0000-0002-8512-2802

Article

Keywords: Arabidopsis thaliana, jasmonic acid, herbivory

Posted Date: August 6th, 2021

DOI: https://doi.org/10.21203/rs.3.rs-148432/v1

Long-lasting memory of jasmonic acid-dependent immunity requires DNA demethylation and ARGONAUTE1

Wilkinson SW[1], Muench A[1], Wilson RS[1], Hooshmand K[2], Henderson MA[1], Moffat EK[1], Stassen JHM[1], López Sánchez A[1], Fomsgaard IS[2], Krokene P[3], Mageroy MH[3] and Ton J[1,*]

[1] Plants, Photosynthesis and the Rhizosphere Cluster, School of Biosciences, Institute for Sustainable Food, The University of Sheffield, Sheffield S10 2TN, United Kingdom

[2] Department of Agroecology, Aarhus University, DK-4200 Slagelse, Denmark

[3] Division for Biotechnology and Plant Health, Norwegian Institute of Bioeconomy Research (NIBIO), 1433 Ås, Norway

*Correspondence: j.ton@sheffield.ac.uk

ABSTRACT

Stress can alter important plant life-history traits. Here, we report the long-term effects of the stress hormone jasmonic acid (JA) on the defence phenotype, transcriptome and DNA-methylome of Arabidopsis. Three weeks after transient JA signalling activity, 5-week-old plants retained induced resistance (IR) against herbivory but showed enhanced susceptibility to necrotrophic and biotrophic pathogens. Transcriptome analysis of these plants revealed priming and/or up-regulation of JA-dependent defence genes but repression of ethylene- and salicylic acid-dependent genes. Long-term JA-IR against herbivory was associated with shifts in glucosinolate composition and required MYC2/3/4 transcription factors, DNA (de)methylation pathways and the small RNA (sRNA)-binding protein ARGONOUTE1 (AGO1). Although methylome analysis did not reveal consistent changes in DNA methylation near MYC2/3/4-controlled genes, JA-treated plants were specifically enriched with hypomethylated *ATREP2* transposable elements (TEs), while *ATREP2*-derived sRNAs showed increased association with AGO1. Our results indicate that AGO1-associated sRNAs from hypomethylated *ATREP2* TEs *trans*-regulate long-lasting memory of JA-dependent immunity.

INTRODUCTION

To resist pests and diseases, plants have evolved wide-ranging strategies which unfold over different timescales[1]. Pattern-triggered immunity (PTI) is an immediate immune response that protects against most attackers. However, specialised pests and diseases can suppress PTI, enabling them to initiate a parasitic interaction with their hosts[2–4]. The residual basal resistance is too weak to arrest specialised attackers but contributes to slowing down their colonisation[5]. Moreover, specific environmental signals can augment basal resistance. This so-called induced resistance (IR) is mediated by prolonged upregulation and/or priming of PTI-related defences[1], as PTI, basal resistance and IR share similar signalling pathways[3,5,6]. The defence hormones salicylic acid (SA) and jasmonic acid (JA) play central roles in these pathways[6,7]. While SA-dependent defences are mostly effective against (hemi-)biotrophic pathogens, JA activates defences against both necrotrophic pathogens and herbivores[3,7,8].

The immediate effects of JA signalling on defence gene expression are well documented. In *Arabidopsis thaliana* (Arabidopsis), bio-active JA-isoleucine (JA-Ile) stimulates binding of the F-box protein COI1 to JAZ repressor proteins[9–11]. This molecular interaction leads to ubiquitin-dependent degradation of JAZ proteins, which in turn results in induced activity of the defence regulatory transcription factors (TFs) MYC2/MYC3/MYC4 (MYC2/3/4) and EIN3/EIL3[9,11–14]. The MYC2/3/4 and EIN3/EIL1 branches of the JA response pathway are co-regulated by the plant hormones abscisic acid (ABA) and ethylene (ET), directing the JA pathway towards activation of defences against herbivory or necrotrophic pathogens, respectively[3,7,13,15–18].

Compared to the short-term effects of JA, little is known about the long-term impacts of JA, despite the potential impacts transient stress responses can have on ecologically relevant life-history traits, such as growth rate, seed set and immune responsiveness[1]. It has been reported that treatment of Arabidopsis with methyl jasmonate (MeJA) elicits transgenerational IR against chewing herbivores[19], suggesting an epigenetic basis of long-

term JA-IR. However, the epigenetic mechanisms underpinning long-term JA-IR and their associated impacts on global gene expression remain poorly understood.

In plants, cytosine (C) methylation occurs at three sequence contexts: CG, CHG and CHH (H being any base other than G) and predominantly targets transposable elements (TEs) to silence their potentially damaging effects on the genome[20]. The establishment of methylation at TE-rich regions is under antagonistic control by RNA-directed DNA methylation (RdDM)[21,22] and the DNA demethylase ROS1[20,23]. Over recent years, evidence has emerged that RdDM and ROS1 regulate plant defences against biotic stress[24–26].

Here, we have investigated the long-term effects of JA on the defence-related phenotype, transcriptome and DNA methylome of Arabidopsis. We show that long-lasting JA-IR at 3 weeks after treatment of 2-week-old seedlings is effective against herbivory but not against pathogens. The response is associated with shifts in the defence-related transcriptome and metabolite profiles and is dependent on the MYC2/3/4 branch of the JA response pathway, RdDM- and ROS1-dependent DNA (de)methylation pathways, and the small RNA (sRNA)-binding effector protein ARGONAUTE1 (AGO1). Global DNA methylome sequencing furthermore showed that long-term JA-IR is associated with highly specific hypomethylation of TEs from the *ATREP2* family, while analysis of AGO1-associated sRNAs revealed increased association with sRNAs from this TE family. We propose a novel model of long-lasting plant immune memory, involving *ATREP2*-derived small interfering RNAs (siRNAs) that augment MYC2/3/4-dependent resistance through nuclear AGO1.

RESULTS

JA induces long-term resistance to a generalist herbivore and long-term susceptibility to both necrotrophic and hemi-biotrophic pathogens.

To examine the dynamics of the JA response over an extended time period, 2-week-old Arabidopsis seedlings were treated with water or 1mM JA and analysed for JA-dependent *MYC2* and *VSP2* expression over a 3-week period (Fig. 1a,b). Both marker genes showed transient induction at 4 and 24 hours (hrs) post seedling treatment, after which their expression reverted to near baseline levels by 1 to 3 weeks (Fig. 1b). To assess the long-term effects of this transient JA signalling activity on the defence phenotype, we quantified resistance in 5-week-old plants, at 3 weeks after seedling treatment, against the generalist herbivore *Spodoptera littoralis* (*Sl*), the necrotrophic fungus *Plectosphaerella cucumerina* (*Pc*) and the biotrophic bacterial pathogen *Pseudomonas syringae* pv. *tomato* DC3000 (*Pst*; Fig. 1a). To compare these long-term effects with the short-term effects of JA, we also challenged an additional batch of 5-week-old plants with the same stresses at 1 day after treatment with water or 1 mM JA (Fig. 1a). As expected, the short-term effects of JA were characterised by IR against both *Sl* and *Pc*, as evidenced by a statistically significant reduction in larval weight and lesion diameter, respectively (Fig. 1c). Furthermore, JA treatment 1 day before *Pst* challenge increased bacterial leaf multiplication (Fig. 1c), supporting earlier reports that JA signalling suppresses SA-dependent resistance against biotrophic pathogens[27,28]. Interestingly, even though JA signalling activity had reverted to near basal levels at 1 week after JA seedling treatment (Fig. 1b), 5-week-old plants from JA-treated seedlings retained IR against *Sl* and induced susceptibility (IS) to *Pst* (Fig. 1d). Whereas, in contrast to the short-term JA response, plants from JA-treated seedlings displayed IS to the necrotrophic fungus *Pc* (Fig. 1d), indicating a fundamental difference between the short- and long-term effects of JA on Arabidopsis immunity. To verify the biological relevance of these contrasting long-term effects of JA on *Sl* and *Pc* resistance, we subjected seedlings to transient feeding by *Sl* larvae, which induces JA accumulation[29]. As

observed after JA seedling treatment, seedling exposure to *Sl* feeding elicited long-term IR against *Sl* and long-term IS to *Pc* (Extended Data Fig. 1). Hence, the long-term effects of transient JA signalling activity at the seedling stage are biologically relevant and phenotypically different to the short-term JA response.

JA seedling treatment induces long-term priming of JA-dependent defences against herbivory but represses SA- and JA/ET-dependent defences against pathogens.

Since *MYC2* and *VSP2* expression reverted to near basal levels by 3 weeks after JA seedling treatment (Fig. 1b), we hypothesised that long-term JA-IR against *Sl* is based on priming of JA-dependent defence genes. To test this, we quantified expression of MYC-dependent anti-insect acid phosphatase gene *VSP2* at 4, 8 and 24 hrs after challenging leaves from seedling-treated plants with water or 0.1 mM JA. Plants from JA-treated seedlings showed strongly augmented *VSP2* induction after JA challenge, confirming that JA seedling treatment causes long-term priming of antiherbivore defences (Fig. 1e). Conversely, plants from JA-treated seedlings showed reduced responsiveness of the SA-inducible antimicrobial *PR1* gene after challenge with 0.1 mM SA, as well as the JA/ET-dependent antifungal *PDF1.2* gene after challenge with a mixture of 0.1 mM JA + 0.1 mM of the ethylene precursor 1-aminocyclopropanecarboxylic acid (ACC; Fig. 1e). Hence, JA seedling treatment induces long-lasting priming of JA-inducible *VSP2* but long-term repression of SA-induced *PR1* and JA/ET-inducible *PDF1.2*.

Long-term impacts of JA seedling treatment on the transcriptome.

To assess the long-term impacts of JA on a global transcriptome level, we performed mRNA sequencing (mRNA-seq) of leaves from 5-week-old plants of water- and JA-treated seedlings at 4 hrs after challenge with water or JA (Fig. 1e). Principal component analysis (PCA; Fig. 2a) and hierarchical cluster analysis (HCA; Fig. 2b) of normalised and transformed read counts revealed clear separation of samples by (pre)treatment (n=4; water seedling treatment and water challenge = W_W, JA seedling treatment and water challenge

= JA_W, water seedling treatment and JA challenge = W_JA and JA seedling treatment and JA challenge = JA_JA). Hence, JA treatment of seedlings had a profoundly different impact on the transcriptome than JA challenge treatment of 5-week-old plants.

Since JA seedling treatment altered the resistance/susceptibility to JA-eliciting attackers (Fig. 1d), we hypothesised that JA seedling treatment modifies transcriptional responsiveness to secondary JA challenge. Accordingly, we selected genes showing a statistically significant interaction between JA seedling treatment and JA challenge (FDR-adjusted *p*-value < 0.01). The resulting 2,409 genes showed a range of different expression patterns (Extended Data Fig. 2 and Supplementary Data 1). To select for genes that are specifically associated with long-term JA-IR against *Sl*, we filtered the 2,409 genes for those that (i) were upregulated upon JA challenge in plants from water-treated seedlings (W_JA > W_W) and (ii) showed augmented expression after JA challenge in plants from JA-treated seedlings compared to plants from water-treated seedlings (JA_JA > W_JA; Supplementary Data 2). HCA of the resulting 832 genes revealed four clusters, of which two (II and IV) displayed long-term upregulation and/or primed JA responsiveness in plants from JA-treated seedlings (Extended Data Fig. 3a and Fig. 2c). The 203 genes in clusters II and IV included the *VSP2* marker gene and were statistically enriched with gene ontology (GO) terms related to herbivore resistance, particularly “glucosinolate biosynthetic process” (Extended Data Fig. 3b, Fig. 2d and Supplementary Data 3, 4 and 5). To select genes associated with long-term JA-IS to *Pst*, we filtered the 2,409 genes for those which (i) were downregulated in response to JA challenge in plants from water-treated seedlings (W_JA < W_W) and (ii) showed reduced expression after JA challenge in plants from JA-treated seedlings compared to plants from water-treated seedlings (JA_JA < W_JA; Supplementary Data 6). HCA of the resulting 904 genes revealed three clusters, of which two (V and VI) showed consistent short- and long-term repression by JA (Extended Data Fig. 3a and Fig. 2c). GO enrichment analysis of the 796 genes in clusters V and VI indicated enrichment of terms related to biotrophic pathogen resistance, including SA signalling (Extended Data Fig. 3b, Fig. 2d and

Supplementary Data 7, 8 and 9). Finally, to select genes associated with long-term JA-IS to *Pc*, we filtered the 2,409 genes for those which (i) were upregulated in response to JA challenge in plants from water-treated seedlings (W_JA > W_W) and (ii) reduced in expression after JA challenge in plants from JA-treated seedlings compared to plants from water-treated seedlings (JA_JA < W_JA, Supplementary Data 10). HCA of the resulting 395 genes revealed one cluster (IX) with 144 genes showing long-term repression by JA and significant enrichment with numerous GO terms related to necrotrophic pathogen resistance (Extended Data Fig.3, Fig. 2c,d and Supplementary Data 11, 12 and 13). Thus, JA seedling treatment induces long-term priming/upregulation of genes related to JA-dependent defence against herbivores and long-term repression of SA- and ET-dependent genes against biotrophic and necrotrophic pathogens.

Long-term JA-IR against herbivory is dependent on MYC2/3/4 transcription factors.

To further investigate the transcriptional regulation of long-term JA-IR against *Sl*, we analysed the promoters of the 203 IR-related genes for statistical enrichment with TF DNA binding motifs (1 kb upstream from transcriptional start site; TSS). Most strongly enriched motifs contained the canonical G-box motif (CACGTG; Fig. 3a and Supplementary Data 14), which functions as a core binding site for bHLH TFs, including JA regulatory TFs MYC2/3/4 (Fig. 3a and Supplementary Data 14)[17,30,31]. To validate involvement of MYC2/3/4 in long-term JA-IR against herbivory, we compared long- and short-term JA-IR against *Sl* in 5-week-old Col-0 and the *myc2 myc3 myc4* triple mutant (*mycT*)[17]. As reported previously[17,32], water-treated *mycT* plants allowed significantly higher larval growth than water-treated Col-0 plants (Fig. 3b), reflecting their compromised basal resistance against herbivory. Furthermore, JA-treated Col-0 plants allowed significantly lower rates of larval growth than water-treated Col-0 plants, confirming their ability to express short- and long-term JA-IR against *Sl* (Fig. 3b). By contrast, JA treatment of *mycT* elicited neither short- nor long-term JA-IR against *Sl* (Fig. 3b), demonstrating a critical role of MYC2/3/4 TFs in both IR responses to this herbivore. Notably, *mycT* and Col-0 plants displayed similar reductions in plant growth after JA seedling

treatment (Extended Data Fig. 4), indicating that long-term JA-IR is unrelated to JA-induced growth repression.

Long-term JA-IR against herbivory requires intact DNA (de)methylation pathways.

The defence-related phenotypes at 3 weeks after JA seedling treatment were expressed in leaves that were not present at the seedling stage, suggesting that there is a self-perpetuating resistance signal which is transmitted through cell division into the newly formed leaves. Changes in DNA methylation offer a plausible mechanism, since these can be transmitted through cell division[33]. Furthermore, previous studies have indicated that changes in DNA methylation of TEs controls defence gene expression[25,34]. Since TE methylation in Arabidopsis is controlled by the antagonistic activities of RdDM and the DNA demethylase ROS1[20], we investigated whether this regulatory system is required for JA-IR by testing two previously characterised mutants in RdDM (*nrpe1-11*) and ROS1 (*ros1-4*)[25] for short- and long-term JA-IR against *Sl*. Both mutants expressed similar levels of basal resistance and short-term JA-IR as the wild-type (Col-0; Fig. 4a). By contrast, long-term JA-IR was strongly reduced in *nrpe1-11* and *ros1-4* compared to Col-0 and failed to cause a statistically significant reduction in larval development (Fig. 4a). All genotypes displayed similar reductions in plant growth after JA seedling treatment, indicating that the lack of JA-IR in *nrpe1-11* and *ros1-4* is unrelated to differences in JA-induced growth repression (Extended Data Fig. 4).

To obtain further evidence of the role of RdDM and ROS1 in long-term JA-IR against herbivory, we performed dual-choice assays to detect differences in attractiveness to *Sl* larvae between water- and JA-treated plants. At 20 hrs after release of the larvae in the choice arenas, a significantly higher number of *Sl* larvae preferred water-treated Col-0 plants over JA-treated Col-0 plants, demonstrating that long-term JA-IR reduces the attractiveness to *Sl* (Fig. 4b). By contrast, *nrpe1-11* and *ros1-4* plants from water- and JA-treated seedlings attracted similar numbers of larvae (Fig. 4b), confirming that the *ros1-4* and *nrpe1-11* mutants are similarly affected in long-term JA-IR against herbivory. Since *ROS1* is positively

209 controlled by RdDM via a DNA methylation monitoring sequence within its promoter[20,35], we
210 propose that the phenotypic similarity of *ros1-4* and *nrpe1-11* is caused by reduced *ROS1*
211 expression[25,35].

212 **Long-term JA-IR is associated with ROS1-dependent changes in indole**
213 **glucosinolates.**

214 The 203 genes associated with long-term JA-IR against *Sl* were statistically enriched with
215 genes controlling the biosynthesis of glucosinolates (Fig. 2 and Supplementary Data 1 and
216 5). This suggests that the composition and size of the glucosinolate pool may be altered
217 long-term following JA seedling treatment and contribute to the IR against *Sl*. Furthermore,
218 this alteration could be dependent on changes in DNA methylation. We therefore used high
219 performance liquid chromatography coupled with triple quadrupole mass spectrometry
220 (HPLC-QqQ) to profile changes in glucosinolate content between WT and *ros1-4* plants
221 following JA seedling treatment. JA had long-term effects on glucosinolate composition (Fig.
222 4d,e and Extended Data Fig. 5), predominantly altering concentrations of indole
223 glucosinolates (IGs). The main IG compound, glucobrassicin (I3M), as well as its
224 downstream derivative neoglucobrassicin (NMOI3M), showed a statistically significant
225 increase in WT plants upon JA seedling treatment (Fig. 4d,e). Whereas the IG 4-
226 methoxyglucobrassicin (4MOI3M) was statistically repressed by JA seedling treatment.
227 Interestingly, these long-term changes in IG profiles were strongly attenuated (I3M and
228 NMO13M) or absent (4MOI3M) in the *ros1-4* mutant (Fig. 4e). Hence, ROS1-dependent
229 DNA hypomethylation is not only essential for long-term JA-IR (Fig. 4b,c) but also controls
230 the associated shifts in IG composition (Fig. 4d,e).

231 **The methylome of long-term JA-IR is characterised by variable DNA hypomethylation**
232 **at TEs.**

233 To assess the long-term impacts of JA on global DNA methylation, biologically replicated
234 leaf samples (*n*=3) from 5-week-old plants at 3 weeks after seedling treatment were

analysed by whole-genome bisulfite sequencing (WGBS). For all sequence contexts the genome-wide weighted C methylation levels were comparable to previously reported values[36] (Extended Data Fig. 6a). Furthermore, although JA-treated samples showed on average marginally lower levels of genome-wide weighted C methylation, the differences were not statistically significant for any sequence context (Extended Data Fig. 6a). PCA and HCA of C methylation did not indicate consistent directional effects of JA seedling treatment. However both analyses revealed strongly increased variation in C methylation between replicate samples of JA-treated plants (Fig. 5a,b), which was driven by CHG and CHH sequence contexts (Fig. 5b and Extended Data Fig. 6b). Since non-CG methylation mostly occurs at intergenic TE sequences[37], we hypothesised that the increased variation in DNA methylation in plants from JA-treated seedlings occurs at TEs. To test this hypothesis, we selected differentially methylated regions (DMRs) between each individual JA replicate and all 3 water replicates (1JA_vs_3W). In contrast to statistical comparisons between 3 replicates from each treatment (3JA_vs_3W), which selects for DMRs that are consistently different across replicate JA samples, the 1JA_vs_3W comparisons allows for identification of statistically significant DMRs that are variable between replicate JA samples. For DNA methylation at all sequence contexts (all-C), the three 1JA_vs_3W comparisons identified 325, 291 and 260 DMRs, respectively (Fig. 5c and Supplementary Data 15 and 16). Although these DMRs were relatively small (average 41 bp), they were C-rich (average 13 C/DMR) and showed substantial shifts in C methylation (average difference in methylation level of 43 percentage points; Supplementary Data 16). The 1JA_vs_3W comparisons for CHH context identified an average of 588 DMRs (Fig. 5c and Supplementary Data 15 and 16), while the comparisons for CHG and CG contexts yielded only 52 and 28 DMRs, respectively (Fig. 5c and Supplementary Data 15 and 16). These sequence-specific DMRs were also relatively small (average 53, 50 and 42 bp for CHH, CHG and CG, respectively) with substantial changes in C methylation (average difference of 45, 37 and 41 percentage points for CHH, CHG ad CG, respectively; Supplementary Data 16). Notably, the majority of DMRs across all contexts and comparisons overlapped with TEs at intergenic regions and

263 were hypomethylated in plants from JA-treated seedlings (Fig. 5c and Supplementary Data
264 16). Hence, the long-term variation in DNA methylation by JA seedling treatment is largely
265 driven by variable hypomethylation of TEs at non-CG context.

266 **Long-term JA-IR is not associated with *cis*-acting DMRs within promoters of**
267 **differentially expressed defence genes.**

268 DNA methylation in gene promoters can influence the binding of TFs to gene promoters
269 motifs[20,38], which supports previous studies that have linked changes in gene expression
270 and/or responsiveness to differential DNA methylation of the corresponding
271 promoters[24,25,35,39]. Although our global WGBS analysis suggests that JA-induced changes in
272 DNA methylation occur at variable locations (Fig. 5a,b and Extended Data Fig. 6b), we
273 examined whether DMRs from the different 1JA_vs_3W comparisons cluster within wider
274 consensus regions of the same promoter regions. To this end, we searched for regions
275 encompassing three DMRs, one from each of the 1JA_vs_3W comparisons (for details, see
276 Methods). At all-C context, we identified 2 consensus DMRs, which mapped to the same
277 region on chromosome 1 and were not located at gene promoters (Supplementary Data 17).
278 Increasing the maximum distance between individual DMRs from 100 to 500 bp did not yield
279 additional consensus DMRs (Supplementary Data 17). Furthermore, we did not identify
280 consensus DMRs at CG or CHG contexts and only identified 10 and 25 consensus DMRs at
281 CHH context, using 100 and 500 bp maximum gaps, respectively (Supplementary Data 17).
282 Although 7 and 19 of the latter CHH consensus DMRs were located within gene promoters,
283 including *WRKY14* (AT1G30650), *GAT1* (AT1G08230) and *CAM7* (AT3G43810,
284 Supplementary Data 17), none of these genes were differentially expressed in our
285 transcriptome analysis (Supplementary Data 1). We therefore conclude that the regulatory
286 role of RdDM and ROS1 in long-term JA-IR (Fig. 4) does not stem from *cis*-acting DMRs in
287 promoters of MYC2/3/4-dependent defence genes.

288 **The *ATREP2* TE family is specifically targeted for long-term hypomethylation by JA**
289 **seedling treatment.**

Recent evidence suggests that DNA hypomethylation of TEs can stimulate defence gene expression via *trans*-regulatory mechanisms[1,34,40], offering an alternative mechanism by which RdDM- and ROS1-dependent methylation controls long-term JA-IR. Various *trans*-acting mechanisms have been proposed, including activities by TE-derived small interfering RNAs (siRNAs)[1]. In the case of long-term JA-IR, however, such *trans*-regulating siRNAs would unlikely be generated by the same set of hypomethylated TEs, since there were only a few consensus DMRs between plants from JA-treated seedlings (Supplementary Data 17). Since TEs within the same family and/or related families are highly homologous[41], we hypothesised that different TEs from the same taxonomic family can have similar *trans*-acting activities. To test this hypothesis, we first mined our data for TE (super)families that are significantly enriched with JA-induced DMRs. Strikingly, the *Helitron* TE family *ATREP2* stood out with on average a 11-fold (all-C) and 8-fold (CHH) enrichment with JA-induced DMRs compared to the genomic background of all TEs, which was highly significant for all 1JA_vs_3W comparisons at all-C and CHH contexts (Fig. 5d,e). These *ATREP2* DMRs were mostly hypomethylated and spread evenly across all chromosomes (Extended Data Fig. 7), but none were part of consensus DMRs in the proximity of differentially expressed defence genes (Supplementary Data 1 and 17). Apart from *ATREP2*, there were a small number of additional TE families that were weakly enriched at JA-induced CHH DMRs (Fig. 5e and Extended Data Fig. 8a), but they did not show the same fold-enrichment and statistical significance as *ATREP2*, nor were they consistently enriched across all three 1JA_vs_3W all-C context comparisons (Fig. 5d,e and Extended Data Fig. 8a,b). For JA-induced DMRs at CG and CHG contexts, there was weak enrichment of the *Gypsy* superfamily of LTR retrotransposons (Extended Data Fig. 8c,d). However, this enrichment was borderline statistically significant and did not translate to enrichment of specific TE families (Extended Data Fig. 8c,d). Thus, despite the variation in DNA hypomethylation, JA seedling treatment consistently targets TEs from the *ATREP2* family. Combined with the observed up-regulation and/or priming of MYC2/3/4-dependent defence genes (Figs. 2 and 3) and the critical role of RdDM- and ROS1-dependent DNA methylation in long-term JA-IR (Fig. 4), our WGBS

results suggest that stochastic hypomethylation of members from the *ATREP2* TE family induce and/or prime JA-dependent defence genes via *trans*-acting mechanisms.

AGO1 associates with siRNAs derived from *ATREP2* TEs and is essential for long-term JA-IR against herbivory.

Recently, Liu and colleagues (2019) reported that AGO1 associates with sRNAs in the nucleus and stimulates JA-dependent defence gene expression by changing the genes' chromatin structure and recruiting Pol-II[42]. To examine whether sRNAs from hypomethylated *ATREP2* TEs play a role in long-term JA-IR by associating with AGO1, we mined previous sequencing data of RNAs associated with AGO1 immunoprecipitated from nuclear extracts of MeJA-treated Arabidopsis[42]. To enrich for AGO1-associated siRNAs, RNA sequences from other known RNA classes were removed from the analysis. As is shown in Fig. 6a, *ATREP2*-derived sRNAs showed strongly increased association with AGO1 compared to sRNAs from two similarly sized class 2 families (*ATREP7* - 164 members and *TNAT1A* - 162 members, respectively), which were not targeted for hypomethylation.

To confirm the function of AGO1 in long-term JA-IR, we quantified long-term JA-IR in two Arabidopsis lines carrying relatively weak mutant alleles of *AGO1* (*ago1-45* and *ago1-46*)[43], which were not majorly affected in growth and development. While the weight of *Sl* larvae reared on WT plants from JA-treated seedlings was significantly reduced compared to larvae reared on naïve WT plants, this long-term JA-IR was absent in *ago1-45* and *ago1-46* plants (Fig. 6b). Hence, long-term JA-IR requires an intact AGO1 protein. Together, these results indicate that siRNAs from hypomethylated *ATREP2* associate with nuclear AGO1 to prime and/or upregulate distant JA-dependent defence genes and mediate long-term JA-IR (Fig. 6c).

DISCUSSION

The immediate signalling response to JA has been studied extensively[44]. As a result, the pathways controlling short-term JA-IR against herbivores and necrotrophic pathogens, as well as the antagonistic effects of JA signalling on SA-dependent resistance against biotrophic pathogens, are well-documented[7,27,28]. By contrast, the long-term impacts of JA-dependent stress signalling have largely been overlooked, which does not do justice to the full breath of plant adaptive strategies. Our study shows that the long-term response to JA is phenotypically and mechanistically distinct from the short-term response (Fig. 1), involving changes in DNA methylation of TEs and the sRNA-binding protein AGO1 (Fig. 4-6).

IR is typically based on a combination of priming and prolonged upregulation of inducible defences[1]. The 203 genes associated with long-term JA-IR showed long-term priming and/or prolonged upregulation after JA seedling treatment (Fig. 2c). Consistent with the IR phenotype against *Sl*, this gene set included genes with previously reported anti-herbivore activity (e.g.*VSP1* and *VSP2*)[45] and was statistically enriched with GO terms related to glucosinolate biosynthesis (Fig. 2d and Supplementary Data 4 and 5). Subsequent HPLC-QqQ profiling of glucosinolates confirmed that plants expressing long-term JA-IR show significant changes in IG composition (Fig. 4d,e and Extended Data Fig. 5). Previous studies have demonstrated that these anti-herbivore defences are controlled by MYC2/3/4 TFs[17,32]. Indeed, enrichment analysis of TF DNA-binding motifs in promoters of the 203 IR-related genes revealed strong enrichment with MYC-binding G-box motifs (Fig. 3a)[17,30], while the *mycT* mutant was impaired in long-term JA-IR against *Sl* (Fig. 3b). Hence, the immunological memory of long-term JA-IR is retained at the MYC2/3/4-dependent branch of the JA pathway, resulting in priming and/or prolonged up-regulation of anti-herbivore genes.

Recent evidence points to an important role of DNA methylation in plant immunity[24–26,34,40,46]. In most studies, however, epigenetic resistance phenotypes are induced by artificial gene mutations affecting DNA methylation, which does not necessarily demonstrate biological relevance. By contrast, our study has shown that transient signalling activity by the plant's

368 own stress hormone or caterpillar infestation induces immune memory against herbivory,
369 which is transmitted and maintained in newly developed leaves and dependent on RdDM
370 and the DNA demethylase ROS1 (Fig. 4). Since DNA methylation of TEs is tightly controlled
371 by RdDM and ROS1[20,23], these results indicate that long-term JA-IR requires changes in the
372 methylation status of TEs. Although RdDM and ROS1 have opposite effects on DNA
373 methylation, their shared function in long-term JA-IR could be explained by the RdDM-
374 activated DNA methylation monitoring sequence in the promoter of the *ROS1* gene[20,35]. This
375 'methylstat' allows for negative feedback on excessive DNA methylation, ensuring tightly
376 regulated homeostasis of TE activities. Our finding that long-term JA-IR is associated with
377 genome-wide changes in non-CG methylation at TEs (Fig. 5c) supports the involvement of
378 this regulatory system.

379 Biotic stress typically leads to genome-wide DNA hypomethylation in plants[1,20,47]. For
380 instance, both *Pst* infection and SA treatment induce wide-spread hypomethylation in the
381 genome of Arabidopsis[48,49], while MeJA treatment has been reported to induce DNA
382 demethylation in *Brassica rapa*[50]. In most cases, this stress-induced DNA hypomethylation is
383 enriched at TE sequences[1,47,48,51,52], which supports our finding that the vast majority of JA-
384 induced occurred at TEs in non-CG context (Fig. 5c). However, in contrast to previous
385 studies, our WGBS analysis revealed considerable variability in TE hypomethylation by JA.
386 Furthermore, the few consensus DMRs in our dataset were not located near the MYC2/3/4-
387 dependent defence genes that were differentially expressed at 3 weeks after JA seedling
388 treatment. Considering the critical role of RdDM and ROS1 in long-term JA-IR (Fig. 4), we
389 propose that a variable pool of hypomethylated TEs can *trans*-stimulate the expression
390 and/or responsiveness of MYC2/3/4-dependent defence genes to mediate long-term JA-IR
391 (Figs. 2c,d and 3). This notion is supported by independent studies suggesting that
392 hypomethylated TEs *trans*-regulate the expression and/or responsiveness of defence
393 genes[1,25,34,40].

394 Different mechanisms have been proposed for *trans*-regulation of defence genes by
395 hypomethylated TEs, including changes in long-range heterochromatic interactions and
396 activities by TE-derived siRNAs[1,46]. Evidence in support of the latter mechanism comes from
397 the recent discovery that siRNA-associated AGO1 stimulates JA-dependent defence gene
398 expression through interaction with the SWI/SNF chromatin-remodelling complex and
399 recruitment of Pol-II[42]. Interestingly, two independent mutations in AGO1 blocked long-term
400 JA-IR against *Sl* (Fig. 6b). In addition, we found that long-term JA-IR is specifically
401 associated with hypomethylated DMRs at TEs of the *ATREP2* family (Fig. 5d), which
402 generate siRNA sequences that show increased association with nuclear AGO1 (Fig. 6a).
403 Together, these results provide plausible evidence that prolonged up-regulation and priming
404 of defence genes during long-term JA-IR is controlled by AGO1-associated siRNAs from
405 hypomethylated *ATREP2* TEs (Fig. 6c). As homologous members of the same TE family can
406 generate similar siRNAs, this model also explains how variable patterns of DNA
407 hypomethylation result in the same IR phenotype. Accordingly, our study has uncovered a
408 novel mode of epigenetic stress memory in plants.

METHODS

Plant materials and growth conditions.

All Arabidopsis genotypes used in this study are in the genetic background of the accession Columbia (Col-0). The *ros1-4* (SALK_135293), *ago1-45* (NASC ID = N67861) and *ago1-46* (NASC ID = N67862) mutants were obtained from the Nottingham Arabidopsis Stock Centre (NASC) and the *nrpe1-11* (SALK_029919) mutant was kindly provided by Professor Pablo Vera (Instituto de Biología Molecular y Celular de Plantas, Spanish National Research Council, Spain). Seeds of *ros1-4* and *nrpe1-11* came from stocks that had previously been confirmed to carry the correct T-DNA insertions and display transcriptional knock-down of *ROS1* and *NRPE1* genes, respectively[25]. *ago1-45* and *ago1-46* seed stocks were confirmed to be the correct genotype using previously described derived cleaved amplified polymorphic sequences (dCAPS) assays[43]. The *myc2 myc3 myc4* triple mutant (*mycT*)[17] was kindly provided by Professor Roberto Solano (Centro Nacional de Biotecnología, Consejo Superior de Investigaciones Científicas (CNB-CSIC), Spain). Seeds were stored at 4 °C in the dark and suspended in deionised H_2O (dH_2O) for 4 days to break dormancy, after which they were sown onto soil consisting of Scott's Levington M3 compost (Everris) and sand in a 3:1 ratio and cultivated under the following conditions: 8.5:15.5 hr day:night, 21 °C, 45-70% relative humidity (RH) and 100-250 µE m^{-2} s^{-1}.

Pathogen strains and cultivation.

Plectosphaerella cucumerina strain *BMM* (*Pc*) was kindly provided by Professor Brigitte Mauch-Mani (University of Neuchâtel, Switzerland). *Pc* was continuously cultured on potato dextrose agar (PDA) in the dark and at 15-25 °C. Four weeks prior to spore collection, a plug of *Pc* PDA was transferred to a new plate. *Pseudomonas syringae* pv. *tomato* DC3000 *luxCDABE* (*Pst*) was kindly provided by Dr Jun Fan (John Innes Centre, UK)[53]. Glycerol stocks of *Pst* were stored at -80 °C. Two days prior to inoculation, a glycerol stock was

thawed on ice and then cultured at 28 °C on King's B (KB) agar plates supplemented with rifampicin (50 μg ml^{-1}) and kanamycin (50 μg ml^{-1}).

Insect rearing.

Spodoptera littoralis (*Sl*) eggs were kindly provided by Professor Ted Turlings (University of Neuchatel, Switzerland). Larvae were reared in-house on a semi-artificial diet, which was formulated based on the diets in refs.[54–56]. A full diet ingredient list is provided in Supplementary Table 1. The diet was prepared by autoclaving the agar in half the volume of water (300 ml) and then mixing with the additional ingredients.

Chemical treatments.

Stock solutions were prepared by diluting jasmonic acid (JA; Sigma Aldrich, J2500), 1-aminocyclopropanecarboxylic acid (ACC; Sigma Aldrich, A3903) and salicylic acid (SA; Sigma Aldrich, S3007) in absolute ethanol (JA and SA; Fisher Scientific, E/0650DF/17) or dH_2O (ACC). Solutions for plant treatments were prepared by diluting stocks with dH_2O and supplementing with 0.02% of the surfactant silwet L-77 (LEHLE SEEDS, VIS-30). Pre-treatment was performed with 1 mM JA. Challenge consisted of 0.5 mM SA, 0.1 mM JA or 0.1 mM JA + 0.1 mM ACC. The controls for both the pre-treatment ('control') and challenge ('mock') consisted of dH_2O supplemented with the same percentage ethanol as in the corresponding hormone solution. Pre-treatments were performed with either 2-week-old seedlings (long-term experiments; 3 weeks prior to challenge) or nearly 5-week-old plants (short-term experiments; 1 day prior to challenge). Challenge treatments were performed when plants were 5 weeks old. All chemical treatments were performed by spraying plants until the leaf surfaces were entirely covered by liquid.

Seedling treatment by herbivory.

To test the long-term effects of transient seedling exposure to herbivory, 2nd instar *Sl* larvae were placed on 2-week-old Col-0 plants and allowed to feed until 50-75% of above ground tissue had been removed. To prevent (lethal) damage to the hypocotyl and encourage larvae

460 to feed from the cotyledons and leaves, soil was piled around the hypocotyl and a 15 ml
461 falcon tube was placed over each plant. These protective measures were also applied to
462 control plants without larvae.

463 **Quantification of IR against necrotrophic *Pc*.**

464 Four leaves of the same developmental stage on 5-week-old plants (17-22 plants per
465 treatment-genotype combination) were droplet-inoculated with 6 µl droplets of *Pc* inoculum
466 (5×10^6 spores/ml H_2O), as described previously[57,58]. Inoculated plants were maintained at
467 100% RH. Lesion diameters were measured at 6-8 days post inoculation (dpi) and averaged
468 into a single value per plant (unit of biological replication).

469 **Quantification of IR against hemi-biotrophic *Ps*.**

470 Four leaves of the same developmental stage on 5-week-old plants (9-12 plants per
471 treatment-genotype combination) were syringe-infiltrated with a 10 mM $MgSO_4$ suspension
472 containing *Pst* bacteria at OD_{600nm} = 0.0002[59]. Plants were maintained at 80-100% RH. At 3
473 dpi, 4 leaf disks (0.2 cm^2) were harvested per plant and pooled (unit of biological replication).
474 Leaf discs were homogenised in 10 mM $MgSO_4$ and 5-fold dilution series were plated on KB
475 agar plates supplemented with rifampicin (50 µg ml^{-1}) and kanamycin (50 µg ml^{-1}). Plates
476 were incubated at 28 °C for 20 hrs and 4 °C for 17 hrs prior to colony counting. Colonisation
477 was expressed as the number of colony forming units (cfu's) per cm^2 of leaf tissue.

478 **Quantification of IR against *Sl*.**

479 To quantify larval growth in no-choice assays, 5-week-old plants (15-24 plants per treatment-
480 genotype combination) were grown individually in 425 ml transparent plastic cups with three
481 0.8 cm^2 holes drilled in the bottom to allow for water drainage. A single *Sl* neonate larva was
482 placed on each plant with a fine paintbrush and a transparent lid was placed on each cup.
483 Larvae were removed and weighed when complete consumption of the most susceptible
484 phenotype was imminent or after 7 days, whichever came first. The weight of a single larva
485 fed on an individual plant represented the unit of biological replication.

To quantify herbivore attractiveness in dual-choice assays, 5-week-old plants were placed in the dual-choice arenas (18 per genotype) at 3 weeks after seedling treatment. Every arena consisted of two plants from water- or JA-treated seedlings of the same genotype, which were in separate pots positioned in a 1 L transparent plastic container backfilled with soil and separated by a 30 mm inverted Petri dish lid (the 'arena'). Five 2nd-3rd instar *Sl* larvae were placed into the arena, after which containers were closed with pin-pricked lids. After 20 hrs, the position of each larva was recorded. If larvae were not on a plant or the soil immediately under it, they were recorded as not making a choice.

Hyperspectral quantification of plant size.

Five-week-old plants (22-24 per treatment-genotype combination) were imaged, using a PlantScreen HC 900 hyperspectral imaging system (Photon Systems Instruments), consisting of a push-broom scanner with a halogen lamp light source and complementary metal-oxide-semiconductor detector (spatial resolution = 1,000 pixels and spectral resolution = 0.8 nm) mounted on a motorised carriage, which travelled directly over trays of plants at 15 mm s^{-1}. The camera lens was positioned 20 cm above the rosettes and a 0.09 s exposure time was used. Raw intensity values were acquired for 480 wavebands across a 350-900 nm spectral range.

Plant size was approximated based on rosette surface area (RSA), which was quantified as the number of pixels in an image associated with one plant (unit of biological replication). Segmentation of plants from their background was achieved using a four-step pipeline. (i) A calibrated reflectance image (R) was produced, with reflectance values for all wavebands and pixels being generated using the following equation:

$$(1) \qquad R = \frac{I_{Raw} - I_{dark}}{I_{light} - I_{dark}}$$

The intensity values were taken from one raw hyperspectral image (I_{raw}) and two reference images of the same white Teflon standard, one of which was taken in the light (I_{light}) and one in complete darkness (I_{dark}). (ii) The wider area of the calibrated image containing the plant of

512 interest was defined. (iii) All pixels within the defined area with a plant index (equation 2) >
513 0.53 were selected.

514 (2) $$Plant\ index = 1.2\big(2.5(R_{740} - R_{672}) - 1.3(R_{740} - R_{556})\big)$$

515 (iv) Approximately one layer of pixels was removed from the edge of each selection of plant-
516 associated pixels ('plant mask'). Computational analyses of the hyperspectral photos were
517 performed with PlantScreen Data Analyser software (Photon Systems Instruments) and R
518 (v3.6.1).

519 **RNA extractions.**

520 Two-week-old WT plants were treated with either water (control) or JA. A subset of plants
521 were challenged 3 weeks later with a water (mock) or chemical solution (JA, SA, or JA +
522 ACC), as detailed above. Leaf material was harvested both before and at 4 hrs, 24 hrs, 1
523 week and 3 weeks after seedling treatment (Fig. 1b) or at 4, 8 and 24 hrs after challenge
524 treatment (Fig. 1e). For the seedling treatment only experiment (Fig. 1b), 2-6 similarly aged
525 plants from the same tray (4 hrs, 24 hrs and 1 week) or 3-5 leaves of a similar
526 developmental stage from a single plant (3 weeks), were pooled and used as units of
527 biological replication (*n*=2-3). For the seedling treatment + challenge experiments (Fig. 1e), 8
528 similarly aged leaves from 2 plants in the same tray were pooled and used as the units of
529 biological replication (*n*=2-4). Total RNA extractions were performed as described
530 previously[25,34].

531 **Reverse transcriptase-quantitative PCR (RT-qPCR).**

532 Genomic DNA removal and cDNA synthesis were performed as described previously[25,34],
533 using approximately 1 µg of total RNA. The sample mixes were prepared with the Rotor-
534 Gene SYBR Green PCR Kit (Qiagen) and run in a Rotor-Gene Q (Qiagen) real-time PCR
535 cycler. Reactions were run at the following cycling conditions: 1 cycle of 10 mins at 95 °C
536 and 35-40 cycles of 10 seconds at 95 °C and 40 seconds at 60 °C. C_t values were based on
537 'take-off' values calculated by the Rotor-Gene Q 2.3.5 software. C_t values from reactions

538 with primers against *MYC2*, *VSP2*, *PDF1.2* and *PR1* (Supplementary Table 2) were
539 calculated relative to a single calibrator sample, using real-time PCR efficiency values (E+1)
540 of each primer pair. For each sample, the resulting values were normalised to the average
541 values of 3 reference genes, *GAPC2* (*AT1G13440*), *UBC21* (*AT5G25760*) and *MON1*
542 (*AT2G28390*), and normalised against the mean relative expression values of replicates
543 harvested prior to seedling treatment (Fig. 1b) or at 4 hrs after mock challenge of water
544 seedling treated plants (Fig. 1e).

545 **Glucosinolate Profiling**

546 Leaf material for glucosinolate profiling was collected from 5-week-old WT and *ros1-4* plants
547 pre-treated with water (control) or JA (1 mM) as 2-week-old seedlings. Biologically replicated
548 samples (*n*=8) consisted of 8 leaves of similar age collected from 2 plants (4 leaves/plant).
549 Leaf tissue was flash frozen and then lyophilized. Extraction and quantification of
550 glucosinolates was performed as described previously[60]. Briefly, 5 mg of dried tissue was
551 ground to a fine powder. Glucosinolates were extracted by addition of 1 ml of 70 % (v/v)
552 methanol/water solution to the powder, vortexed, heated (5 min), shaken (15 min),
553 centrifuged (5 min at 15000g), and the supernatant was transferred into new tubes. The
554 supernatant was diluted in 100% Milli-Q water, filtered through a 0.22-µm KX syringe filter
555 (PTFE 13-mm diameter; Mikrolab), and injected into the LC-MS/MS system.

556 Samples were analysed in multiple reaction mode (MRM) on an Agilent 1260 Infinity HPLC
557 system (Santa Clara) connected to an AB Sciex 4500 triple-quadrupole trap (QqQ) mass
558 spectrometer (QTRAP/MS; AB Sciex), equipped with electrospray ionization (ESI) source in
559 negative ion mode. For each compound, two MRM-transitions, which showed the best
560 signal-to-noise ratios, were monitored.

561 Chromatographic separation for glucosinolates was performed at 40 ˚C on a reversed-phase
562 Synergi Fusion-RP C18, 80A column (250 mm × 2 mm i.d., 4 µm; Phenomenex) equipped
563 with a Security Guard Cartridge (Phenomenex, KJ0-4282). A binary solvent mixture was

used consisting of water (solvent A) and methanol (solvent B). Both solvents contained 20 mM acetic acid. The flow rate was 0.3 ml/min, and the injection volume 20 µl. The binary gradient was set up as follows: 0-3 min, column equilibration (95% A), 3-10 min, ramping to (80% A), 10-17 min, ramping to (55% A), 17-35 min, ramping to (0% A), 35-38 min, isocratic hold (0% A), 38-38.5 min, ramping back to (95% A), and 38.5-45 min, column re-equilibrating (95% A). All data were collected using ABSciex Analyst software v1.6.2. Quantitation was performed using ABSciex MultiQuant software v3.0.2. Samples were run in a randomized order.

Statistical analysis of data from bioassays, hyperspectral imaging, glucosinolate profiling and RT-qPCR.

All statistical analyses were performed in R v3.6.1. Data from *Ps*, *Pc* and no-choice *Sl* assays, hyperspectral imaging, glucosinolate profiling and RT-qPCR experiments were analysed by linear models. If data showed normal distributions and homoscedasticity, the analysis was performed by two-sample t-tests (binary comparisons) or one-, two- or three-way ANOVAs followed by Tukey post-hoc tests (multiple groups). Welch two-sample t-tests were used when binary comparison data showed heteroscedasticity. If data showed heteroscedasticity and/or residuals did not follow a normal distribution, data were transformed (logged, squared, square-rooted or transformed with the Box-cox or Yeo-Johnson transformations). When transformations failed to yield normal distributions, data were analysed by non-parametric Mann-Whitney tests (binary comparisons) or Kruskal-Wallis tests followed by Pairwise Wilcoxon Rank Sum Tests (multiple groups) with *p*-values adjusted using the FDR approach. In all cases, a difference was deemed statistically significant at $p < 0.05$. To test for statistically significant changes in larval attractiveness in the dual-choice *Sl* assays, total numbers of larvae choosing plants from water- or JA-treated seedings were analysed by a Goodness-of-fit test against the null hypothesis that larval numbers were equal across treatments ($p < 0.05$).

mRNA transcriptome analysis: library preparation and sequencing.

mRNA-sequencing (mRNA-seq) analysis was based on the same total RNA extracts used for RT-qPCR analysis of *VSP2* expression at 4 hrs after water/JA challenge (*n*=4; Fig. 1d). Quantity and quality of RNA was assessed using a Nanodrop and 2100 Bioanalyzer (Agilent Technologies). All RNA extracts used for sequencing yielded RNA integrity numbers (RIN) of at least 6.4. Library preparation and sequencing was performed by BGI Genomics. mRNAs were isolated using an oligo dT-based selection for poly(A) tails. Sequencing was performed with the BGISEQ-500 platform functioning in its single end mode. Across all 16 samples 598 million 50 bp single-end clean reads were generated, with an average of 37.4 million clean reads per sample (Supplementary Data 18). On average 98.7% of nucleotides per sample had a Phred quality score of > 20 (Supplementary Data 18).

mRNA transcriptome analysis: read alignment and counting.

Read quality was assessed using FASTQC v0.11.5 (http://www.bioinformatics.babraham.ac.uk/projects/fastqc/) and MultiQC v1.7[61]. The first 15 bases of reads were removed using the read trimming tool Trimmomatic v0.38 (options: 'SE', 'HEADCROP:15')[62]. Reads were aligned to the Arabidopsis genome (Ensembl Plants vTAIR10.40), using STAR v2.6.1b with default parameters[63]. All samples had read alignment efficiencies between 89.3-90.8% (average 90.3%; Supplementary Data 18). Numbers of reads mapping to each annotated gene were counted using HTSeq v0.9.1 (option: '--stranded=no')[64].

mRNA transcriptome analysis: statistical analysis of the mRNA-seq data.

Read count tables were loaded into R v3.6.1 and genes with a total read count of < 100 across all samples were removed. Read counts were normalised for library size and transformed with a variance stabilising transformation (VST)[65]. Principal component analysis (PCA) of the 16 samples was performed using the 'plotPCA' function from DEseq2 v1.24.0[66] and displayed with ggplot2 v3.2.1. The outcome of hierarchical cluster analysis (HCA) of the

16 samples was displayed using pheatmap v1.0.12, with the complete linkage clustering method and Euclidean distances.

To identify differentially expressed genes (DEGs) associated with long-term JA-induced changes in resistance against JA-eliciting attackers, we used DESeq2[66] to select for expression profiles with a statistically significant interaction between JA seedling treatment and JA challenge treatment. A total of 2,409 DEGs were selected with an FDR-adjusted *p*-value (*p.adj*) < 0.01 (Extended Data Fig. 2). These represented genes that responded differently to JA challenge as a result of JA seedling treatment. The expression profiles were projected in an clustered heatmap by the 'aheatmap' function of NMF v0.21.0, using Ward's method and Pearson correlation distances. VST-transformed count data were projected in the heatmap as per gene z-scores.

To identify DEGs associated with the long-term JA-IR against *Sl*, genes were selected based on their expression profile across the four treatment combinations (W_W, JA_W, W_JA, JA_JA; first letters indicate seedling treatment and second letters challenge treatment). Selected genes had to (i) be upregulated in response to JA challenge in plants from water-treated seedlings (W_JA > W_W) and (ii) exhibit augmented expression after JA challenge in plants from JA-treated seedlings compared to plants from water-treated seedlings (JA_JA > W_JA). A clustered heatmap displaying the resulting 832 genes was created using Ward's clustering method and Spearman distances (Extended Data Fig. 3a). Based on expression profiles and enrichment of gene ontology (GO) terms related to anti-herbivore defences (see below), clusters II and IV with a total of 203 genes were selected for further analysis. This final set of IR-related genes were projected in a clustered heatmap using Ward's clustering method and Pearson distances (Fig. 2c).

DEGs were selected as associated with long-term JA-IS against *Pst* if they (i) were downregulated in response to JA challenge in plants from water-treated seedlings (W_JA < W_W) and (ii) exhibited reduced expression after JA challenge in plants from JA-treated seedlings compared to plants from water-treated seedlings (JA_JA < W_JA). The resulting

643 904 genes were displayed in a clustered heatmap using Ward's clustering method and
644 Pearson distances (Extended Data Fig. 3a). Based on expression profiles and enrichment of
645 GO terms relating to anti-pathogen defences (see below), clusters V and VI with a total of
646 796 genes were selected and displayed in a clustered heatmap created as before (Fig. 2c).

647 DEGs were selected as being associated with long-term JA-IS against *Pc* if they (i) were
648 upregulated in response to JA challenge in plants from water-treated seedlings (W_JA >
649 W_W) and (ii) showed reduced expression after JA challenge in plants from JA-treated
650 seedlings compared to plants from water-treated seedlings (JA_JA < W_JA). The resulting
651 395 genes were displayed in a clustered heatmap using the average clustering method and
652 Spearman distances (Extended Data Fig. 3a). Based on expression profile and enrichment
653 of GO terms relating to anti-pathogen defences (see below), cluster IX with a total of 144
654 genes was selected and displayed in a clustered heatmap created as before (Fig. 2c).

655 **mRNA transcriptome analysis: statistical enrichment analyses of gene ontology terms**
656 **and TF DNA-binding motifs.**

657 GO term enrichment analysis was performed with R packages clusterProfiler v3.12.0 and
658 org.At.tair.db v3.8.2. For analysis of single and multiple gene clusters, the clusterProfiler
659 functions 'compareCluster' and 'enrichGO', respectively, were used with parameters:
660 'universe = all genes with ≥ 100 counts across all 16 samples', 'fun = "enrichGO"'
661 ('compareCluster' only), 'OrgDb = 'org.At.tair.db'', 'keyType = "TAIR"', 'ont = 'BP'',
662 'minGSSize = 10' and 'maxGSSize = 500'. Biological process GO terms with a *p.adj* < 0.05
663 were classed as enriched. Fold enrichment plots of selected enriched defence-related GO
664 terms were created using the R package ggplot2.

665 For the TF DNA-binding motif enrichment analysis, promoter sequences (TSS to 1 kb
666 upstream) for all genes analysed by DESeq2 (≥ 100 reads across all samples), were
667 downloaded from TAIR v10. These promoter sequences, together with the 803 Arabidopsis
668 TF DNA-binding motifs found in the MotifDb v1.26.0 R package and the functions

669 'makePriors', 'PFMtoPWM' and 'makeBackground' from the PWMEnrich v4.20.0 R package,
670 were used to create background distributions of TF DNA-binding motifs. To determine which
671 of the 803 MotifDb Arabidopsis motifs were significantly overrepresented ($p < 0.01$) in the
672 203 IR-related genes promoters relative to the background, the PWMEnrich functions
673 'motifEnrichment' (all parameters default apart from 'group.only = F') and 'groupReport' (all
674 options default) were used. Sequence logos were produced using the PWMEnrich 'plot'
675 function.

676 **Methylome analysis: library preparation and sequencing.**

677 Leaf material for whole-genome bisulphite sequencing (WGBS) analysis was collected from
678 5-week-old plants that had been treated with water (control) or JA as 2-week-old seedlings.
679 Biologically replicated samples (n=3) consisted of 12 leaves of similar age collected from 6
680 plants per tray (2 leaves/plant). Genomic DNA was extracted using the GenElute Plant
681 Genomic DNA Miniprep Kit (Sigma-Aldrich). Library preparation and sequencing was
682 performed by BGI Genomics and their standard WGBS protocol. The sequencing of 150 bp
683 paired-end reads was performed with a HiSeq X Ten System (Illumina). Across all 6
684 samples, 97 million clean paired-end reads were generated, with a minimum and maximum
685 number of 15.6 and 17 million read pairs per sample, respectively (Supplementary Data 19).
686 On average, 98.2% of all nucleotides yielded a Phred quality score of > 20 (Supplementary
687 Data 19).

688 **Methylome analysis: read alignment.**

689 Read quality was assessed using FASTQC and MultiQC[61]. The first 10 bases were removed
690 from the start of each read with Trimmomatic (options: 'PE', 'HEADCROP:10')[62]. Reads were
691 aligned to the Arabidopsis genome (Ensembl Plants vTAIR10.40) using bismark v0.21.0[67],
692 run with the default parameter settings which includes the use of Bowtie2 v2.3.4.1[68] for read
693 mapping. Alignment efficiency for each of the 6 samples was between 58-66%
694 (Supplementary Data 19). To remove duplicate reads, BAM alignment files were rearranged

using SAMtools v1.7 (options: 'sort', '-n')[69] and then passed to the Bismark tool 'deduplicate_bismark' (option: '--paired'). Between 23-29% of aligned paired-end reads were removed from each sample in the deduplication procedure. After alignment and deduplication, between 43-51% of all sequenced paired-end reads were retained per sample (Supplementary Data 19).

Methylome analysis: methylation calling and determining weighted methylation levels.

Methylated and total (methylated + unmethylated) read counts per cytosine (C) position were generated using the Bismark tool 'bismark_methylation_extractor' (options: '--paired-end', '--no_overlap', '--ignore_3prime_r2 90', '--comprehensive', '--bedGraph', '--CX', '--cytosine_report'). Per sample bisulfite treatment non-conversion rates were estimated from the unmethylated plastid genome and ranged between 0.37-0.48% across all 6 samples (Supplementary Data 19; non-conversion rate < 2% is considered acceptable[70]). Counts for all C positions in the nuclear genome were used for downstream analysis of genome-wide methylation at all sequence contexts (all-C), as well as for CG, CHG and CHH contexts separately (H indicates any base other than G). Estimates of genome-wide methylation levels were calculated using the weighted methylation level equation in ref.[71].

Methylome analysis: global analysis of positional cytosine methylation.

To detect global shifts in DNA methylation, HCAs and PCAs were conducted for each of the 4 sequence contexts (all-C, CG, CHG and CHH). Both analyses were performed with positional C-methylation data calculated using the site methylation level equation in ref.[71]. All C positions with a coverage < 5 in one or more samples were removed. In addition, positions with a standard deviation of methylation lower than or equal to the median of the standard deviations of all cytosines across the whole genome were removed, thereby focusing the analyses on the most variable positions. PCAs were conducted with the R function 'prcomp' (options: 'center = TRUE', 'scale = FALSE'). HCA was performed with the R functions 'dist' and 'hclust' run with the options 'method = "euclidean"' and 'method = "average"',

721 respectively. PCA and HCA plots were created with the R packages ggplot2 v3.6.1 and
722 dendextend v1.13.4.

723 **Methylome analysis: analysis of differentially methylated regions.**

724 Since the global methylome analyses revealed increased variation in C methylation between
725 replicate samples from plants of JA-treated seedlings, we adjusted our strategy for statistical
726 selection of differentially methylated regions (DMRs) by selecting for DMRs that were
727 statistically different between each individual sample from JA-treated plants and all three
728 replicate samples from water-treated plants (1JA_vs_3W). This approach is not confounded
729 by the increased variability between JA samples. To identify DMRs in each of the three all-C
730 context 1JA_vs_3W comparisons, we used the DSS v2.26.0 R package functions 'DMLtest'
731 (options: 'equal.disp = TRUE', 'smoothing = FALSE') followed by 'callDMR' (options: 'delta =
732 0.1', 'p.threshold = 0.05', 'minlen = 25', 'minCG = 5', 'dis.merge = 50', 'pct.sig = 0.5')[72,73].
733 Since DSS accounts for coverage depth information, we included all C positions. Context-
734 specific DMRs were identified by running the same DSS analysis pipeline with C positions at
735 CG, CHG or CHH contexts only.

736 To map DMRs to genomic features, Arabidopsis genome and TE annotation files were
737 downloaded from Ensembl vTAIR10.40 and TAIR v10, respectively. Analysis of DMRs
738 overlapping with specific genomic features was conducted with the R packages
739 GenomicRanges v1.36.1 and genomation v1.16.0. The precedence order for DMRs
740 overlapping with genomic features was promotor > exon > intron > intergenic. Statistical
741 enrichment of TE (super)families within DMRs was determined by hypergeometric tests,
742 using all TEs annotated in TAIR v10 as the background ($p.adj < 0.05$). Plots of DMR
743 frequencies and TE (super)family enrichments were created using the R packages ggplot2
744 and ggrepel v0.8.1. A chromosome map displaying the distribution of DMR-overlapped
745 *ATREP2* TEs was generated using the TAIR v10 gaps track downloaded from the UCSC
746 genome browser, the centromere coordinates obtained from the TAIR v9 genome assembly
747 and the R package chromPlot v1.12.0.

Consensus DMRs were defined as wider regions encompassing one DMR from each of the three 1JA_vs_3W comparisons, and were selected using the following pipeline: (i) identified 'overlapping' DMRs from a pair of 1JA_vs_3W comparisons, using the 'findOverlaps' function from the R package GenomicRanges, (ii) created merged DMRs using the highest and lowest coordinates from across the DMR pair, (iii) identified DMRs from the third 1JA_vs_3W comparison which "overlapped" merged DMRs, using the 'findOverlaps' function, (iv) created consensus DMRs using the highest and lowest coordinates from across the three DMRs, (v) repeated steps i to iv three times to cover each possible combination of 1JA_vs_3W comparisons, and (vi) removed consensus DMR duplicates. The consensus DMR identification pipeline was run twice for each of the 4 sequence contexts (all-C, CG, CHG and CHH). In the first run, pairs of DMRs were classed as "overlapping" if they were within 100 bp of one another and in the second run if they were within 500 bp of one another.

Analysis of sRNAs associated with nuclear AGO1

Raw sequencing reads of AGO1-associated RNAs from 10-day-old Col-0 at 1 hr after MeJA treatment were downloaded from the NCBI Sequence Read Archive (SRR5313816). For full details on the experimental design and sequencing see Liu et al.[42].

Adaptors were trimmed from reads and low-quality reads were removed using Trim Galore v0.6.2 (options: '--quality 0', '--length 18', '--max_length 30', '--stringency 6', '--max_n 0'). Quality of the remaining reads was assessed using FASTQC and MultiQC[61]. Reads were mapped to the Arabidopsis genome (Ensembl Plants vTAIR10.40) using Bowtie v1.3.0 (options: '-v 0', '--all', '--best', '--sam', '--no-unal'), with all alignments with no mismatches being reported. To focus the analysis on siRNAs plausibly involved in the *trans*-regulation of JA-dependent defence genes by hypomethylated TEs, SAMtools v1.7[69], bedtools v2.30.0[74] and Picard v2.24.2 were used to remove reads mapping to known classes of RNAs (rRNAs, rRNAs, snRNAs, snoRNAs and miRNAs). Subsequently the same tools were used to calculate the number and size of sRNAs mapping to TEs of the *ATREP2*, *ATREP7* and

775 *TNAT1A* families. Coordinates of known classes of RNAs and TEs annotated in the
776 Arabidopsis genome were downloaded from TAIR v10. An sRNA size against frequency
777 distribution plot was created with the R package ggplot2.

DATA AVAILABILITY

The mRNA-seq and WGBS data discussed in this publication have been deposited in NCBI's Gene Expression Omnibus and are accessible through GEO SuperSeries accession number GSE163271 (https://www.ncbi.nlm.nih.gov/geo/query/acc.cgi?acc=GSE163271, reviewer access token: odifuiiopdijxgx). The sRNA-seq data featured in this publication was downloaded from the NCBI Sequence Read Archive (SRR5313816).

REFERENCES

1. Wilkinson, S. W. *et al.* Surviving in a Hostile World: Plant Strategies to Resist Pests and Diseases. *Annu. Rev. Phytopathol.* **57**, 505–529 (2019).

2. Irieda, H. *et al.* Conserved fungal effector suppresses PAMP-triggered immunity by targeting plant immune kinases. *Proc. Natl. Acad. Sci. U. S. A.* **116**, 496–505 (2019).

3. Erb, M. & Reymond, P. Molecular Interactions Between Plants and Insect Herbivores. *Annu. Rev. Plant Biol.* **70**, 527–557 (2019).

4. Pel, M. J. C. & Pieterse, C. M. J. Microbial recognition and evasion of host immunity. *J. Exp. Bot.* **64**, 1237–1248 (2013).

5. Ahmad, S., Gordon-Weeks, R., Pickett, J. & Ton, J. Natural variation in priming of basal resistance: From evolutionary origin to agricultural exploitation. *Mol. Plant Pathol.* **11**, 817–827 (2010).

6. Bigeard, J., Colcombet, J. & Hirt, H. Signaling mechanisms in pattern-triggered immunity (PTI). *Mol. Plant* **8**, 521–539 (2015).

7. Pieterse, C. M. J., Van der Does, D., Zamioudis, C., Leon-Reyes, A. & Van Wees, S. C. M. Hormonal modulation of plant immunity. *Annu. Rev. Cell Dev. Biol.* **28**, 489–521 (2012).

8. Glazebrook, J. Contrasting mechanisms of defense against biotrophic and necrotrophic pathogens. *Annu. Rev. Phytopathol.* **43**, 205–227 (2005).

9. Thines, B. *et al.* JAZ repressor proteins are targets of the SCFCOI1 complex during jasmonate signalling. *Nature* **448**, 661–665 (2007).

10. Sheard, L. B. *et al.* Jasmonate perception by inositol-phosphate-potentiated COI1-JAZ co-receptor. *Nature* **468**, 400–407 (2010).

11. Howe, G. A., Major, I. T. & Koo, A. J. Modularity in Jasmonate Signaling for

808 Multistress Resilience. *Annu. Rev. Plant Biol.* **69**, 387–415 (2018).

809 12. Chini, A., Gimenez-Ibanez, S., Goossens, A. & Solano, R. Redundancy and specificity
810 in jasmonate signalling. *Curr. Opin. Plant Biol.* **33**, 147–156 (2016).

811 13. Zhu, Z. *et al.* Derepression of ethylene-stabilized transcription factors (EIN3/EIL1)
812 mediates jasmonate and ethylene signaling synergy in Arabidopsis. *Proc. Natl. Acad.*
813 *Sci. U. S. A.* **108**, 12539–12544 (2011).

814 14. Chini, A. *et al.* The JAZ family of repressors is the missing link in jasmonate signalling.
815 *Nature* **448**, 666–671 (2007).

816 15. Anderson, J. P. *et al.* Antagonistic Interaction between Abscisic Acid and Jasmonate-
817 Ethylene Signaling Pathways Modulates Defense Gene Expression and Disease
818 Resistance in Arabidopsis. *Plant Cell* **16**, 3460–3479 (2004).

819 16. Bodenhausen, N. & Reymond, P. Signaling Pathways Controlling Induced Resistance
820 to Insect Herbivores in Arabidopsis. *Mol. Plant-Microbe Interact. MPMI* **20**, 1406–1420
821 (2007).

822 17. Fernández-Calvo, P. *et al.* The Arabidopsis bHLH transcription factors MYC3 and
823 MYC4 are targets of JAZ repressors and act additively with MYC2 in the activation of
824 jasmonate responses. *Plant Cell* **23**, 701–715 (2011).

825 18. Song, S. *et al.* Interaction between MYC2 and ETHYLENE INSENSITIVE3 modulates
826 antagonism between jasmonate and ethylene signaling in Arabidopsis. *Plant Cell* **26**,
827 263–279 (2014).

828 19. Rasmann, S. *et al.* Herbivory in the previous generation primes plants for enhanced
829 insect resistance. *Plant Physiol.* **158**, 854–863 (2012).

830 20. Zhang, H., Lang, Z. & Zhu, J. K. Dynamics and function of DNA methylation in plants.
831 *Nat. Rev. Mol. Cell Biol.* **19**, 489–506 (2018).

21. Matzke, M. A. & Mosher, R. A. RNA-directed DNA methylation: an epigenetic pathway of increasing complexity. *Nat. Rev. Genet.* **15**, 394–408 (2014).

22. Cuerda-Gil, D. & Slotkin, R. K. Non-canonical RNA-directed DNA methylation. *Nat. Plants* **2**, 16163 (2016).

23. Tang, K., Lang, Z., Zhang, H. & Zhu, J. The DNA demethylase ROS1 targets genomic regions with distinct chromatin modification. *Nat. Plants* **2**, 16169 (2016).

24. Yu, A. *et al.* Dynamics and biological relevance of DNA demethylation in Arabidopsis antibacterial defense. *Proc. Natl. Acad. Sci. U. S. A.* **110**, 2389–2394 (2013).

25. López Sánchez, A., Stassen, J. H. M., Furci, L., Smith, L. M. & Ton, J. The role of DNA (de)methylation in immune responsiveness of Arabidopsis. *Plant J.* **88**, 361–374 (2016).

26. Halter, T. *et al.* The Arabidopsis active demethylase ROS1 cis-regulates defence genes by erasing DNA methylation at promoter-regulatory regions. *Elife* **10**, e62994 (2021).

27. Cui, J. *et al.* Pseudomonas syringae manipulates systemic plant defenses against pathogens and herbivores. *Proc. Natl. Acad. Sci. U. S. A.* **102**, 1791–1796 (2005).

28. Murmu, J. *et al.* Arabidopsis GOLDEN2-LIKE (GLK) transcription factors activate jasmonic acid (JA)-dependent disease susceptibility to the biotrophic pathogen Hyaloperonospora arabidopsidis, as well as JA-independent plant immunity against the necrotrophic pathogen Botryti. *Mol. Plant Pathol.* **15**, 174–184 (2014).

29. Scholz, S. S. *et al.* Mutation of the Arabidopsis calmodulin-like protein CML37 deregulates the jasmonate pathway and enhances susceptibility to herbivory. *Mol. Plant* **7**, 1712–1726 (2014).

30. Lian, T. fei, Xu, Y. ping, Li, L. fen & Su, X. D. Crystal Structure of Tetrameric Arabidopsis MYC2 Reveals the Mechanism of Enhanced Interaction with DNA. *Cell*

Rep. **19**, 1334–1342 (2017).

31. Carretero-Paulet, L. *et al.* Genome-wide classification and evolutionary analysis of the bHLH family of transcription factors in Arabidopsis, poplar, rice, moss, and algae. *Plant Physiol.* **153**, 1398–1412 (2010).

32. Schweizer, F. *et al.* Arabidopsis basic helix-loop-helix transcription factors MYC2, MYC3, and MYC4 regulate glucosinolate biosynthesis, insect performance, and feeding behavior. *Plant Cell* **25**, 3117–3132 (2013).

33. Law, J. A. & Jacobsen, S. E. Establishing, maintaining and modifying DNA methylation patterns in plants and animals. *Nat. Rev. Genet.* **11**, 204–220 (2010).

34. Furci, L. *et al.* Identification and characterisation of hypomethylated DNA loci controlling quantitative resistance in Arabidopsis. *Elife* **8**, e40655 (2019).

35. Williams, B. P., Pignatta, D., Henikoff, S. & Gehring, M. Methylation-Sensitive Expression of a DNA Demethylase Gene Serves As an Epigenetic Rheostat. *PLoS Genet.* **11**, e1005142 (2015).

36. Niederhuth, C. E. *et al.* Widespread natural variation of DNA methylation within angiosperms. *Genome Biol.* **17**, 194 (2016).

37. Cokus, S. J. *et al.* Shotgun bisulphite sequencing of the Arabidopsis genome reveals DNA methylation patterning. *Nature* **452**, 215–219 (2008).

38. O'Malley, R. C. *et al.* Cistrome and Epicistrome Features Shape the Regulatory DNA Landscape. *Cell* **165**, 1280–1292 (2016).

39. Gallego-Bartolomé, J. *et al.* Targeted DNA demethylation of the Arabidopsis genome using the human TET1 catalytic domain. *Proc. Natl. Acad. Sci. U. S. A.* **115**, E2125–E2134 (2018).

40. Cambiagno, D. A. *et al.* Immune receptor genes and pericentromeric transposons as

881 targets of common epigenetic regulatory elements. *Plant J.* **96**, 1178–1190 (2018).

882 41. Wicker, T. *et al.* A unified classification system for eukaryotic transposable elements.
883 *Nat. Rev. Genet.* **8**, 973–982 (2007).

884 42. Liu, C. *et al.* Arabidopsis ARGONAUTE 1 binds chromatin to promote gene
885 transcription in response to hormones and stresses. *Dev. Cell* **44**, 348–361 (2018).

886 43. Smith, M. R. *et al.* Cyclophilin 40 is required for microRNA activity in Arabidopsis.
887 *Proc. Natl. Acad. Sci. U. S. A.* **106**, 5424–5429 (2009).

888 44. Wasternack, C. How Jasmonates Earned their Laurels: Past and Present. *J. Plant*
889 *Growth Regul.* **34**, 761–794 (2015).

890 45. Liu, Y. *et al.* Arabidopsis vegetative storage protein is an anti-insect acid
891 phosphatase. *Plant Physiol.* **139**, 1545–1556 (2005).

892 46. Parker, A. A., Wilkinson, S. W. & Ton, J. Epigenetics: a catalyst of plant immunity
893 against pathogens. *New Phytol.* (2021).

894 47. Deleris, A., Halter, T. & Navarro, L. DNA Methylation and Demethylation in Plant
895 Immunity. *Annu. Rev. Phytopathol.* **54**, 579–603 (2016).

896 48. Dowen, R. H. *et al.* Widespread dynamic DNA methylation in response to biotic
897 stress. *Proc. Natl. Acad. Sci. U. S. A.* **109**, E2183–E2191 (2012).

898 49. Pavet, V., Quintero, C., Cecchini, N. M., Rosa, A. L. & Alvarez, M. E. Arabidopsis
899 displays centromeric DNA hypomethylation and cytological alterations of
900 heterochromatin upon attack by Pseudomonas syringae. *Mol. Plant-Microbe Interact.*
901 **19**, 577–587 (2006).

902 50. Kellenberger, R. T., Schlüter, P. M. & Schiestl, F. P. Herbivore-Induced DNA
903 demethylation changes floral signalling and attractiveness to pollinators in Brassica
904 rapa. *PLoS One* **11**, e0166646 (2016).

905 51. Atighi, M. R., Verstraeten, B., De Meyer, T. & Kyndt, T. Genome-wide DNA
906 hypomethylation shapes nematode pattern-triggered immunity in plants. *New Phytol.*
907 **227**, 545–558 (2020).

908 52. Hewezi, T. *et al.* Cyst nematode parasitism induces dynamic changes in the root
909 epigenome. *Plant Physiol.* **174**, 405–420 (2017).

910 53. Fan, J., Crooks, C. & Lamb, C. High-throughput quantitative luminescence assay of
911 the growth in planta of Pseudomonas syringae chromosomally tagged with
912 Photorhabdus luminescens luxCDABE. *Plant J.* **53**, 393–399 (2008).

913 54. Gupta, G. P., Rani, S., Birah, A. & Raghuraman, M. Improved artificial diet for mass
914 rearing of the tobacco caterpillar, Spodoptera litura (Lepidoptera: Noctuidae). *Int. J.*
915 *Trop. Insect Sci.* **25**, 55–58 (2005).

916 55. Roeder, K. A., Kuriachan, I., Vinson, S. B. & Behmer, S. T. Evaluation of a microbial
917 inhibitor in artificial diets of a generalist caterpillar, Heliothis virescens. *J. Insect Sci.*
918 **10**, 197 (2010).

919 56. Bricchi, I. *et al.* Separation of early and late responses to herbivory in Arabidopsis by
920 changing plasmodesmal function. *Plant J.* **73**, 14–25 (2013).

921 57. Ton, J. & Mauch-Mani, B. β-amino-butyric acid-induced resistance against
922 necrotrophic pathogens is based on ABA-dependent priming for callose. *Plant J.* **38**,
923 119–130 (2004).

924 58. Pétriacq, P., Stassen, J. & Ton, J. Spore density determines infection strategy by the
925 plant-pathogenic fungus Plectosphaerella cucumerina. *Plant Physiol.* **170**, 2325–2339
926 (2016).

927 59. Yang, L. *et al.* Salicylic acid biosynthesis is enhanced and contributes to increased
928 biotrophic pathogen resistance in Arabidopsis hybrids. *Nat. Commun.* **6**, 7309 (2015).

929 60. Hooshmand, K. & Fomsgaard, I. S. Analytical Methods for Quantification and

930 Identification of Intact Glucosinolates in Arabidopsis Roots Using LC-QqQ(LIT)-
931 MS/MS. *Metabolites* **11**, 47 (2021).

932 61. Ewels, P., Magnusson, M., Lundin, S. & Käller, M. MultiQC: Summarize analysis
933 results for multiple tools and samples in a single report. *Bioinformatics* **32**, 3047–3048
934 (2016).

935 62. Bolger, A. M., Lohse, M. & Usadel, B. Trimmomatic: a flexible trimmer for Illumina
936 sequence data. *Bioinformatics* **30**, 2114–2120 (2014).

937 63. Dobin, A. *et al.* STAR: ultrafast universal RNA-seq aligner. *Bioinformatics* **29**, 15–21
938 (2013).

939 64. Anders, S., Pyl, P. T. & Huber, W. HTSeq-A Python framework to work with high-
940 throughput sequencing data. *Bioinformatics* **31**, 166–169 (2015).

941 65. Anders, S. & Huber, W. Differential expression analysis for sequence count data.
942 *Genome Biol.* **11**, R106 (2010).

943 66. Love, M. I., Huber, W. & Anders, S. Moderated estimation of fold change and
944 dispersion for RNA-seq data with DESeq2. *Genome Biol.* **15**, 550 (2014).

945 67. Krueger, F. & Andrews, S. R. Bismark: a flexible aligner and methylation caller for
946 Bisulfite-Seq applications. *Bioinformatics* **27**, 1571–1572 (2011).

947 68. Langmead, B. & Salzberg, S. L. Fast gapped-read alignment with Bowtie 2. *Nat.*
948 *Methods* **9**, 357–359 (2012).

949 69. Li, H. *et al.* The Sequence Alignment/Map format and SAMtools. *Bioinformatics* **25**,
950 2078–2079 (2009).

951 70. Stuart, T., Buckberry, S. & Lister, R. Approaches for the Analysis and Interpretation of
952 Whole Genome Bisulfite Sequencing Data. in *Epigenome Editing: Methods and*
953 *Protocols, Methods in Molecular Biology* (eds. Jeltsch, A. & Rots, M. G.) 299–310

(Humana Press, 2018).

71. Schultz, M. D., Schmitz, R. J. & Ecker, J. R. 'Leveling' the playing field for analyses of single-base resolution DNA methylomes. *Trends Genet.* **28**, 583–585 (2012).

72. Feng, H., Conneely, K. N. & Wu, H. A Bayesian hierarchical model to detect differentially methylated loci from single nucleotide resolution sequencing data. *Nucleic Acids Res.* **42**, e69–e69 (2014).

73. Wu, H. *et al.* Detection of differentially methylated regions from whole-genome bisulfite sequencing data without replicates. *Nucleic Acids Res.* **43**, e141 (2015).

74. Quinlan, A. R. & Hall, I. M. BEDTools: A flexible suite of utilities for comparing genomic features. *Bioinformatics* **26**, 841–842 (2010).

ACKNOWLEDGEMENTS

We thank Professor Ted Turlings for providing *Spodoptera littoralis* eggs and Professor Roberto Solano for providing the *myc2 myc3 myc4* triple mutant. We also thank Leonardo Furci, David Pascual-Pardo, Ellie Vinnicombe and David Rapley for assistance with experiments and rearing of *S. littoralis*. The work presented in this publication was supported by a consolidator grant (309944 “Prime-A-Plant”) and a proof-of-concept grant (824985, “ChemPrime”) from the European Research Council to J.T., a Research Leadership Award (RL-2012-042) from the Leverhulme Trust to JT, a BBSRC-IPA grant (BB/P006698/1) to J.T., a PROMOS grant (Promo158) from the German Academic Exchange Service (DAAD) and Freie Universität to A.M. and Research Council of Norway grants (249920 and 249958/F20) to P.K. and M.H.M., respectively.

AUTHOR CONTRIBUTIONS

S.W.W., P.K., M.H.M. and J.T. conceived the idea for the research, which was supervised by J.T. S.W.W. conducted experiments and gathered data with assistance from R.S.W., A.M., M.A.H., A.L.S., E.K.M. and M.H.M. K.H. conducted the LC-MS/MS profiling of glucosinolates with assistance from I.S.F. Data analysis was performed by S.W.W. with assistance from R.S.W., A.M., M.A.H., E.K.M., J.H.M.S., A.L.S., K.H. and J.T. The paper was written by S.W.W. and J.T. with comments and input from all other authors. M.H.M., P.K. and J.T. provided funding for the research.

COMPETING INTERESTS STATEMENT

The authors declare no competing interests.

986 **FIGURES**

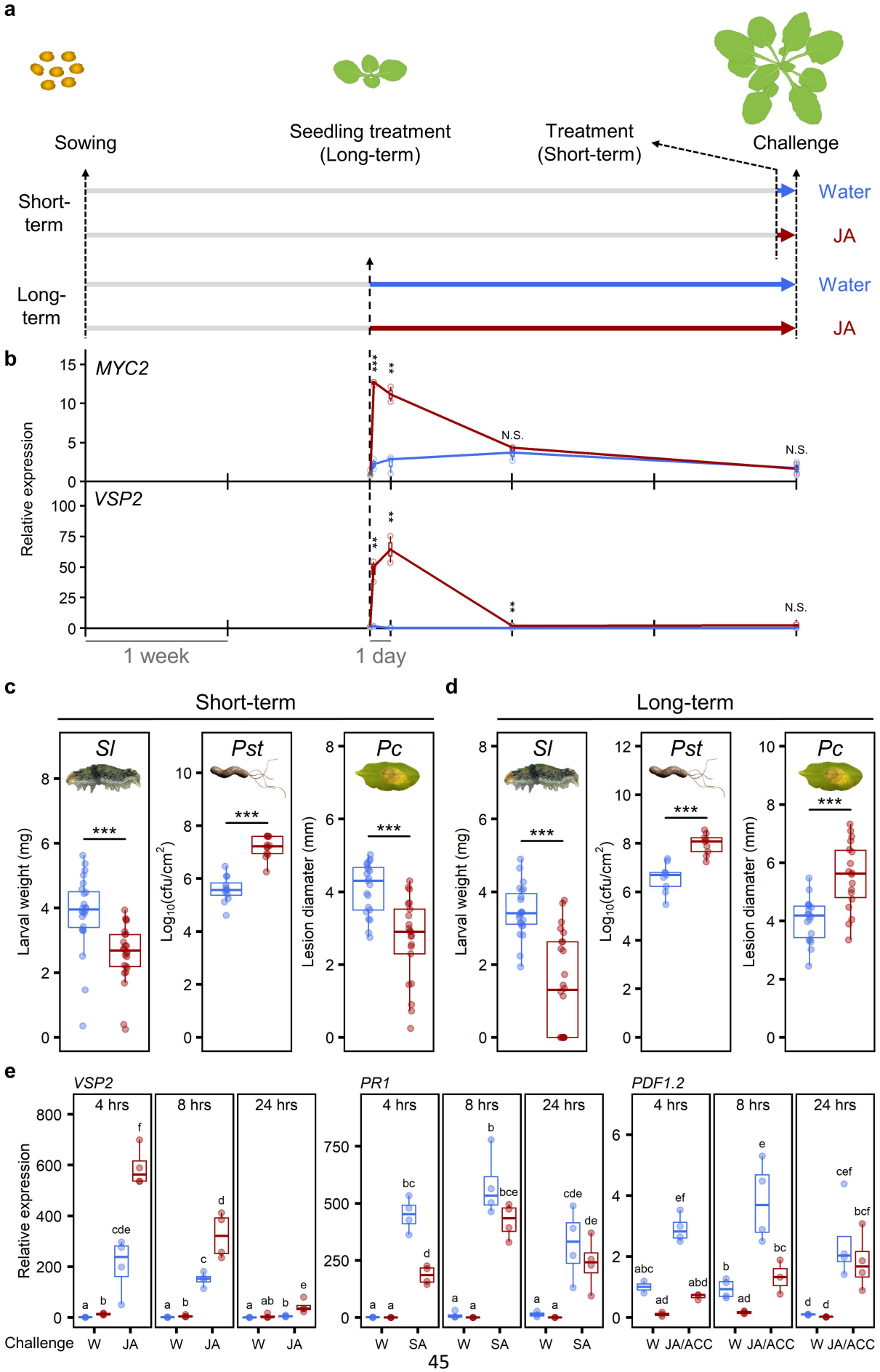
a
Sowing
Seedling treatment (Long-term)
Treatment (Short-term)
Challenge
Short-term
Long-term
Water
JA
Water
JA
b
MYC2
VSP2
Relative expression
N.S.
1 week
1 day
c
Short-term
d
Long-term
Sl
Pst
Pc
Larval weight (mg)
Log10(cfu/cm2)
Lesion diamater (mm)
e
VSP2
PR1
PDF1.2
4 hrs
8 hrs
24 hrs
Relative expression
Challenge
W
JA
SA
JA/ACC

Fig. 1 | Short- and long-term effects of JA on resistance against three different biotic stresses. a, Experimental setup to analyse the short- and long-term impacts of jasmonic acid (JA) on biotic stress resistance in Arabidopsis (Col-0). Plants were pre-treated with water (control, blue) or 1 mM JA (red) at 1 day (short-term) or 3 weeks (long-term) before stress challenge. **b**, Long-term effects of seedling treatments on JA signalling activity over the 3-week period. Shown are the expression profiles (RT-qPCR) of the JA regulatory gene *MYC2* and the JA marker gene *VSP2*. Data points represent gene expression values of biological replicates (n=2-3) relative to the mean expression value of non-treated control plants at the time of seedling treatment (grey). Asterisks indicate statistically significant differences between treatments at individual time-points (Two-sample t-test; N.S. $p > 0.05$, ** $p < 0.01$, *** $p < 0.001$). **c**,**d**, Short- and long-term effects of JA on resistance of 5-week-old plants against the herbivore *Spodoptera littoralis* (*Sl*), biotrophic pathogen *Pseudomonas syringae* pv. *tomato* DC3000 *luxCDABE* (*Pst*) and necrotrophic pathogen *Plectosphaerella cucumerina* (*Pc*). Data points represent weights of individual *Sl* larvae following feeding on individual plants (n=23-34), mean colony forming units (cfu) of *Pst* per cm^2 of leaf tissue per plant (n=9-12) and mean per plant lesion diameters by *Pc* (n=18-21). Asterisks indicate statistically significant differences between pre-treatments (Two-sample t-test for *Pc* and *Pst* assays, Welch two-sample t-test or Mann-Whitney test for *Sl* assays in **c** and **d**, respectively; *** $p < 0.001$). **e**, Long-term effects of JA seedling treatment on the expression of defence marker genes upon challenge with either water (mock) or, 0.1 mM JA (*VSP2*), 0.5 mM salicylic acid (SA; *PR1*) or 0.1 mM JA + 0.1 mM 1-aminocyclopropanecarboxylic acid (ACC; *PDF1.2*). Samples for RT-qPCR analysis were collected at 4, 8 and 24 hours (hrs) after challenge. Data points represent gene expression values of individual replicates (n=2-4) relative to the mean expression values of control plants from water-treated seedlings at 4 hrs post water challenge. Seedling treatment, challenge treatment and harvest timepoint combinations which do not share the same letter are significantly different (Kruskal-Wallis test followed by pairwise Wilcoxon rank sum tests for *VSP2* or ANOVA followed by Tukey post-hoc test for *PDF1.2* and *PR1*; $p.adj < 0.05$). Lower, middle and upper horizontal lines in

1015 boxplots indicate the 1st, 2nd and 3rd quartiles; whiskers extend to the lowest and highest data

1016 points within 1.5 × interquartile range below and above the 1st and 3rd quartiles.

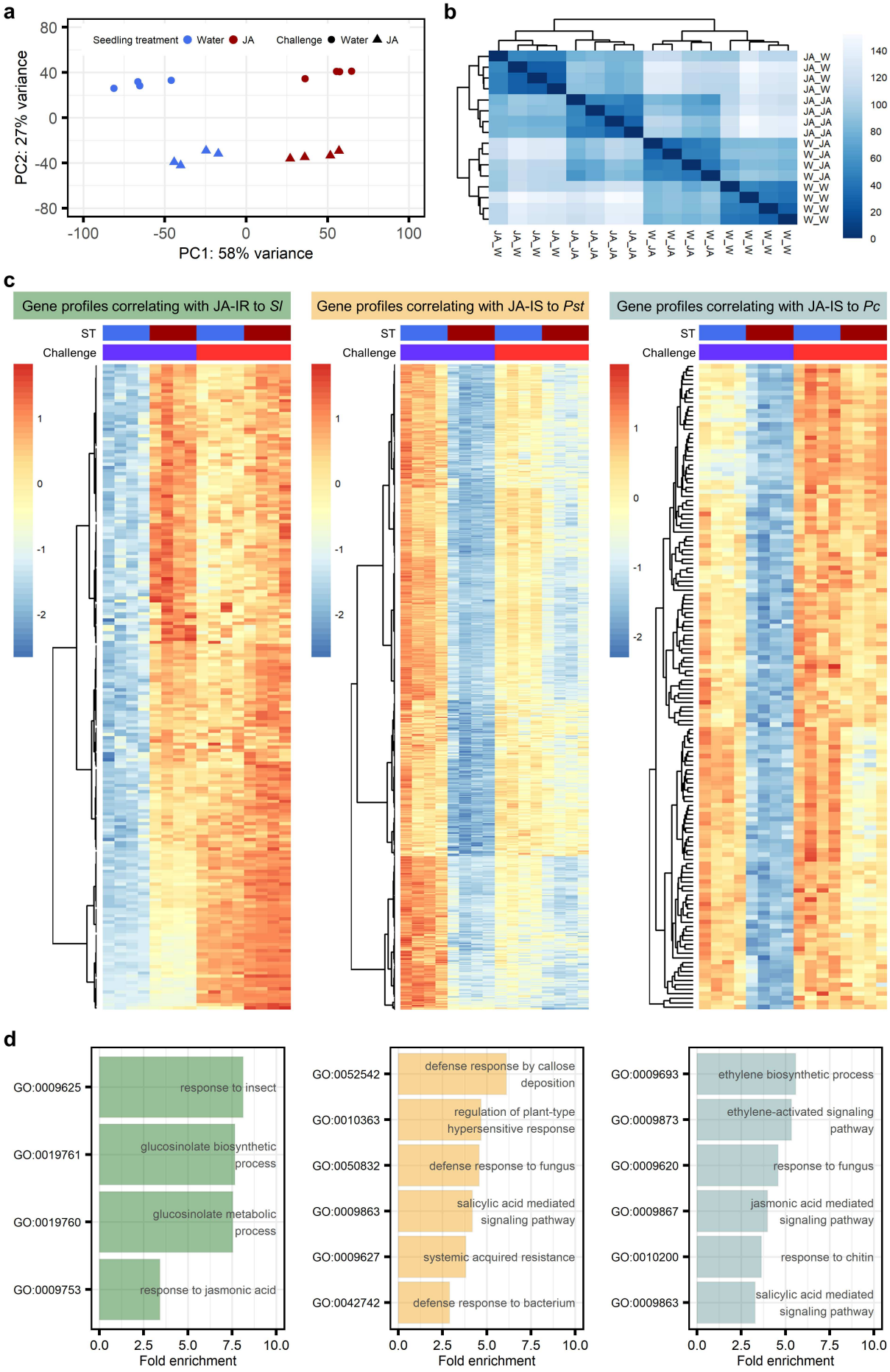
a
Seedling treatment Water JA
Challenge Water JA
PC2: 27% variance
PC1: 58% variance
b
c
Gene profiles correlating with JA-IR to Sl
Gene profiles correlating with JA-IS to Pst
Gene profiles correlating with JA-IS to Pc
ST
Challenge
d
GO:0009625 response to insect
GO:0019761 glucosinolate biosynthetic process
GO:0019760 glucosinolate metabolic process
GO:0009753 response to jasmonic acid
GO:0052542 defense response by callose deposition
GO:0010363 regulation of plant-type hypersensitive response
GO:0050832 defense response to fungus
GO:0009863 salicylic acid mediated signaling pathway
GO:0009627 systemic acquired resistance
GO:0042742 defense response to bacterium
GO:0009693 ethylene biosynthetic process
GO:0009873 ethylene-activated signaling pathway
GO:0009620 response to fungus
GO:0009867 jasmonic acid mediated signaling pathway
GO:0010200 response to chitin
GO:0009863 salicylic acid mediated signaling pathway
Fold enrichment

1017

Fig. 2 | Transcriptome of long-term JA-IR against herbivory and JA-IS against pathogens. a,b, Principal component analysis (PCA) and hierarchical cluster analysis (HCA) of global gene expression patterns, respectively. Samples for mRNA-seq analysis were collected from 5-week-old plants at 4 hrs after challenge with water (W) or 0.1 mM JA. Plants had been pre-treated with water or 1 mM JA at the seedling stage (2-weeks-old). Letters before and after the underscore in the heatmap labels indicate seedling treatment and challenge treatment, respectively. **c**, Transcript profiles of 203, 796 and 144 genes correlating with long-term JA-IR to *Sl*, JA-IS to *Pst* and JA-IS to *Pc*, respectively. Genes are from gene clusters selected based on expression profile and enrichment of biologically relevant GO terms. For details, see text and Extended Data Figs. 2 and 3. Blue and red columns above the heatmaps indicate water and JA treatments, respectively, of seedlings (ST) and 5-week-old plants (Challenge). Heatmap-projected values represent per gene z-scores of transformed read counts from 4 biological replicates for each treatment combination. **d**, Selection of defence-related Gene Ontology (GO) terms enriched within the sets of IR- or IS-related genes ($p.adj < 0.05$). For complete lists of all enriched GO terms, see Supplementary Data 5, 9 and 13.

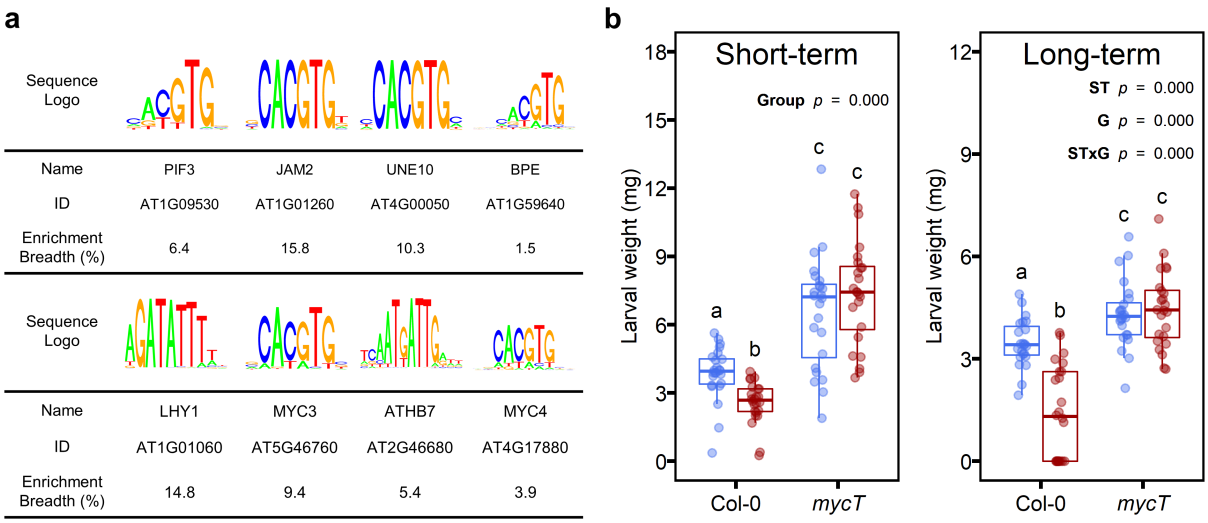

1034 **Fig. 3 | MYC2/3/4 transcription factors control short- and long-term JA-IR against**
1035 **herbivory. a**, Statistical enrichment of transcription factor (TF) DNA binding motifs ($p < 0.01$)
1036 in the 1 kb upstream promoter sequences of the 203 IR-related genes (Fig. 2c). Displayed
1037 are the 8 motifs with the strongest statistical enrichment. Enrichment breadth indicates the %
1038 of promoters for which the motif fell within the top 5% of most strongly enriched motifs.
1039 Name and ID indicate predicted TF binding to the DNA motif. For the complete list of all
1040 statistically enriched DNA motifs, see Supplementary Data 14. **b**, Short- and long-term
1041 effects of water (blue) and 1 mM JA (red) pre-treatment on resistance of 5-week-old WT
1042 (Col-0) and *myc2 myc3 myc4* (*mycT*) plants against herbivory by *Spodoptera littoralis* (*Sl*;
1043 *n*=23-24). Pre-treatment and genotype combinations which do not share the same letter are
1044 significantly different (Kruskal-Wallis test followed by pairwise Wilcoxon rank sum tests for
1045 short-term or ANOVA followed by Tukey post-hoc test for long-term; *p.adj* < 0.05). For more
1046 details, see legend to Fig. 1c,d.

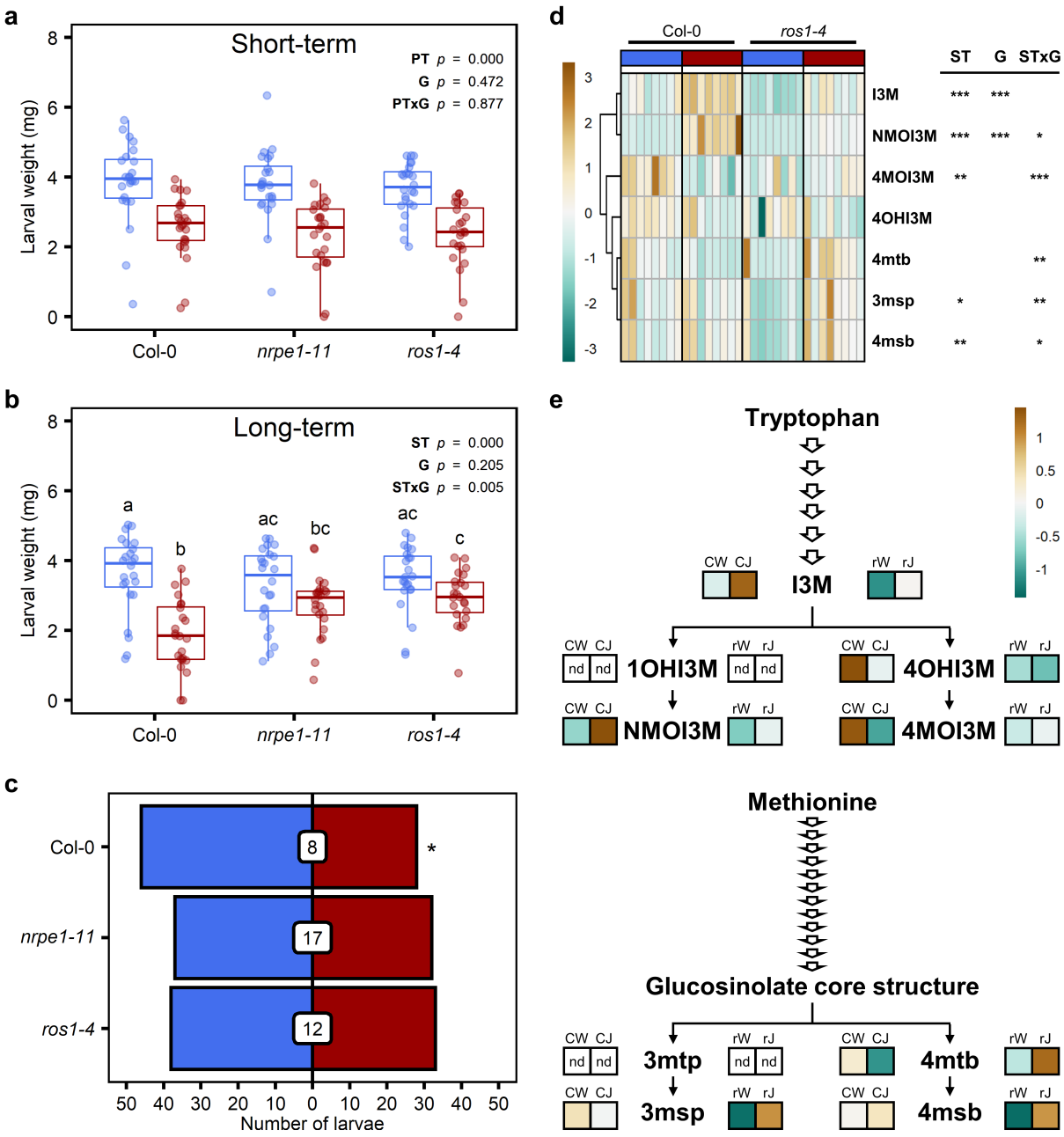

Fig. 4 | Long-term JA-IR against herbivory and associated shifts in glucosinolate profiles require intact DNA methylation homeostasis. a,**b,** Short- (**a**) and long-term (**b**) effects of water (blue) and 1 mM JA (red) pre-treatment on resistance of 5-week-old WT (Col-0) and RdDM (*nrpe1-11*) and ROS1 (*ros1-4*) mutant plants against herbivory by *Spodoptera littoralis* (*Sl*, *n*=23-24). If the pre-treatment (PT) or seedling treatment (ST) x Genotype (G) interaction term was significant (Two-way ANOVA, $p < 0.05$), a Tukey post-doc test was conducted with different letters indicating significant differences between means ($p < 0.05$). For more details, see legend to Fig. 1. **c**, Effects of long-term JA-IR on

attractiveness to *Sl* larvae in dual-choice tests. Shown are the number of larvae preferring 5-week-old plants that had been pre-treated with either water (blue) or 1 mM JA (red) at the seedling stage (2-week-old). White boxes indicate larvae failing to make a choice. Asterisks indicate statistically uneven distributions of larval numbers between treatments (Goodness-of-fit test, * $p < 0.05$). **d**, Long-term effect of water and 1 mM JA on all glucosinolates detected in the leaf tissue of 5-week-old WT and *ros1-4* plants. Heatmap-projected values represent per metabolite z-scores of concentrations (µg/g dry mass) from 8 biological replicates for each genotype-treatment combination. See Extended Data Fig. 5 for raw data. Asterisks indicate significant effects of ST, G or ST x G (Two-way ANOVA, * = $p < 0.05$, ** = $p < 0.01$, *** = $p < 0.001$). **e**, Biosynthesis pathways of indole (top) and aliphatic (bottom) glucosinolates. Heatmap-project values represent z-scores of mean concentrations (µg/g dry mass). CW: Col-0 + water ST, CJ: Col-0 + JA ST, rW: *ros1-4* + water ST, rJ: *ros1-4* + JA ST, nd: not detected, I3M: glucobrassicin, 1OHI3M: 1-hydroxyglucobrassicin, 4OHI3M: 4-hydroxyglucobrassicin, 4MOI3M: 4-methoxyglucobrassicin, NMOI3M: neoglucobrassicin, 3mtp: 3-methylthiopropyl glucosinolate, 3msp: glucoiberin, 4mtb: glucoerucin, 4msb: glucoraphanin.

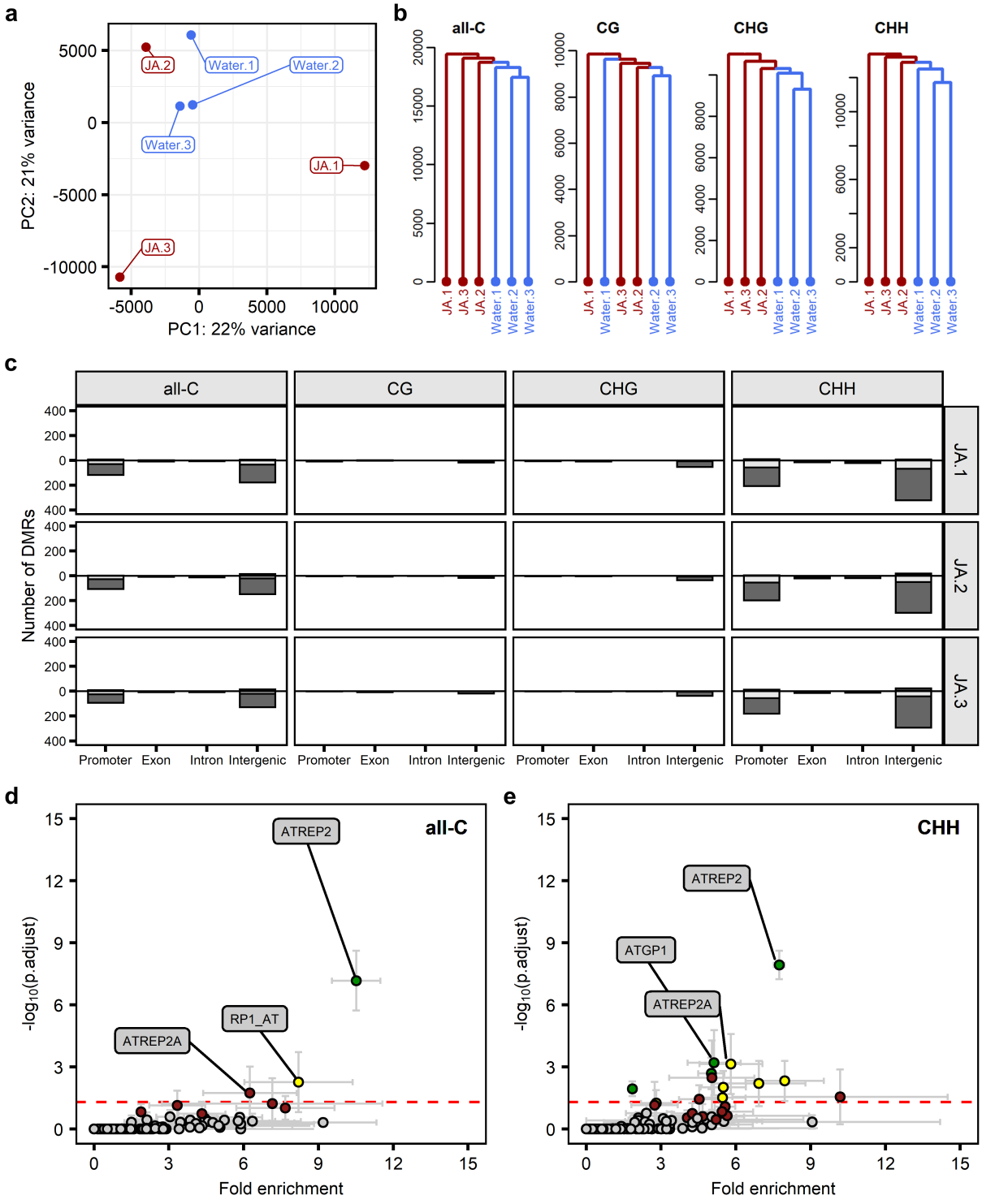

1071 **Fig. 5 | The DNA methylome of long-term JA-IR is associated with selective**
1072 **hypomethylation of *ATREP2* transposable elements.** Biologically replicated leaf samples
1073 (*n*=3) for whole-genome bisulphite sequencing were collected from 5-week-old plants that
1074 had been pre-treated with water or 1 mM JA at the seedling stage (2-week-old). **a**, PCA plot
1075 displaying variation in global cytosine (C) methylation at all-C sequence context between

samples from water (blue) and JA (red) pre-treated plants. **b**, HCA plots displaying global variation in C methylation at all-C, CG, CHG and CHH contexts (H is any nucleotide other than G). **c**, Numbers of differentially methylated regions (DMRs) between individual samples from JA-treated plants (JA.1, JA.2 and JA.3) and all three samples from water-treated plants (1JA_vs_3W comparisons) at gene promoters, exons, introns and intergenic regions. Frequencies of hyper- and hypo-methylated DMRs are indicated by the bars above and below the x-axis, respectively. DMRs at transposable elements (TE) are indicated by dark shading. **d**,**e**, Enrichment of TE families amongst the TEs overlapped by DMRs at all-C and CHH contexts, respectively. Graphs plot statistical enrichment of each TE family against its corresponding fold-enrichment, represented by mean $-\log_{10}(p.adj)$ values (± SEM) and mean fold enrichment values (± SEM), respectively. Enrichment is expressed relative to the background of all genome annotated TEs (TAIR v10). Labelled data points indicate TE families with a mean $-\log_{10}(p.adj) > -\log_{10}(0.05)$ (**d**) or $-\log_{10}(0.001)$ (**e**). Brightly coloured data points indicate TE families that were significantly overrepresented in 1 (red), 2 (yellow) or 3 (green) comparisons, respectively ($p.adj \leq 0.05$). The red dashed line is at $-\log_{10}(0.05)$.

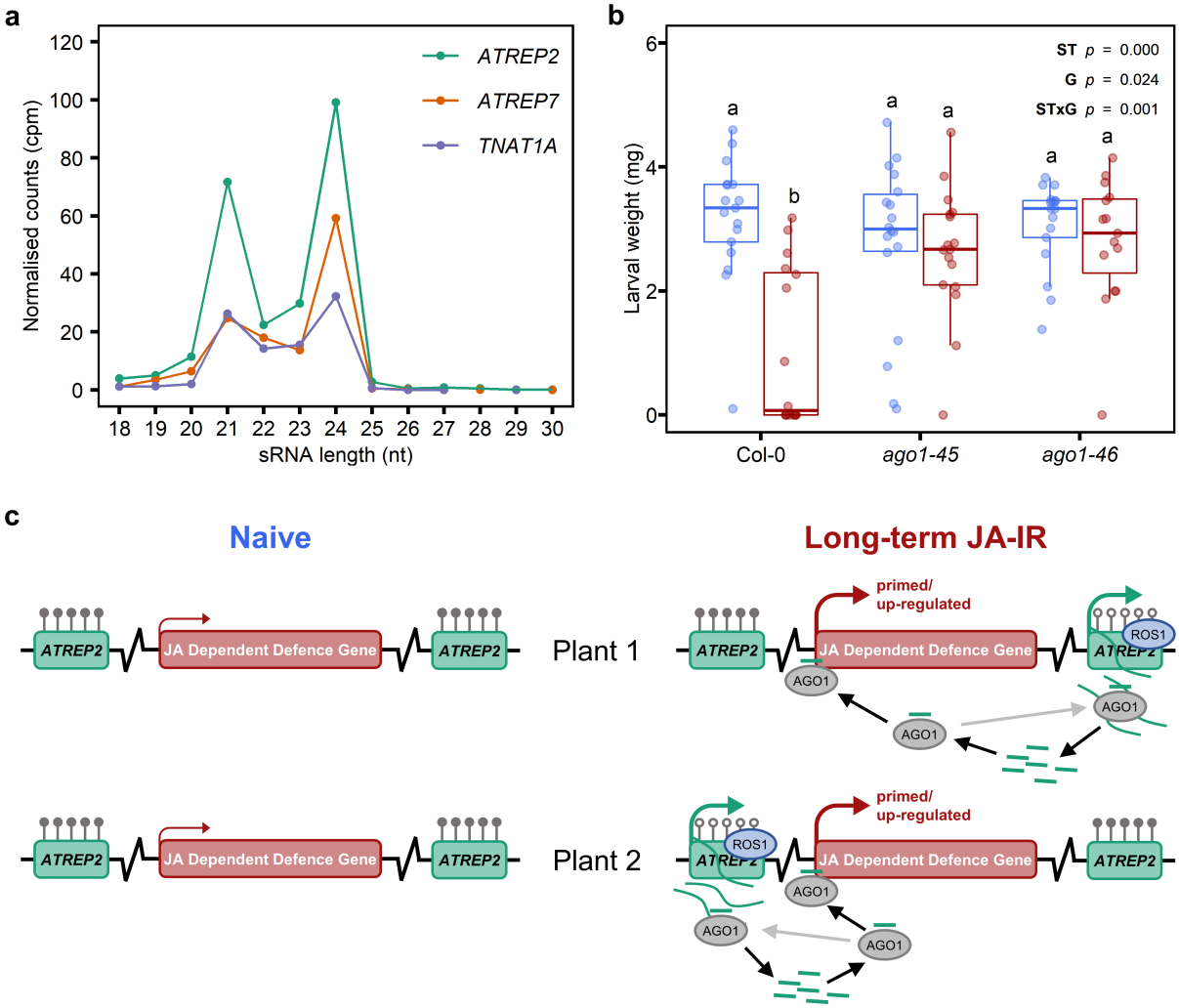

Fig. 6 | AGO1 shows increased association with small interfering RNAs (siRNAs) from *ATREP2* TEs and is essential for long-term JA-IR against herbivory. a, Frequency-size distributions of AGO1-associated small RNAs (sRNAs) mapping to TEs from the *ATREP2* family compared to sRNAs mapping to similarly sized TE families that were not targeted for hypomethylation by JA seedling treatment (*ATREP7* and *NTAT1A*). Nuclear AGO1 was extracted from 10-day-old seedlings at 1 h after treatment with 50 µM MeJA[42]. To enrich the dataset with siRNAs, reads from other known classes of RNAs were excluded from the analysis. All three TE families belong to class 2 and have similar numbers in the Arabidopsis genome (162-164). Counts of sRNAs ranging from 18-30 nucleotides (nt) are displayed as counts per million (cpm) reads. **b**, Long-term effects of water (blue) and 1 mM JA (red) seedling treatment on resistance of 5-week-old WT (Col-0) and *ago1* plants against herbivory by *Spodoptera littoralis* (*Sl*, *n*=15-18). For more details, see legend to Fig. 1. As

the seedling treatment (ST) x Genotype (G) interaction term was significant (Two-way ANOVA, $p < 0.05$), a Tukey post-doc test was conducted, with different letters indicating significant differences between means ($p < 0.05$). **c**, Model of *trans*-regulation of long-term JA-IR by hypomethylated *ATREP2* TEs and AGO1. Following JA seedling treatment, members of the *ATREP2* TE family remain stochastically hypomethylated by ROS1. Hypomethylated *ATREP2* TEs generate transcripts (long curved green lines) that are cleaved by post-transcriptional gene silencing (PTGS) machinery to siRNAs (short green lines) that associate with AGO1. Some siRNA-associated AGO1 proteins associate with the chromatin of distant defence genes, where they recruit Pol-II to upregulate and/or prime expression.

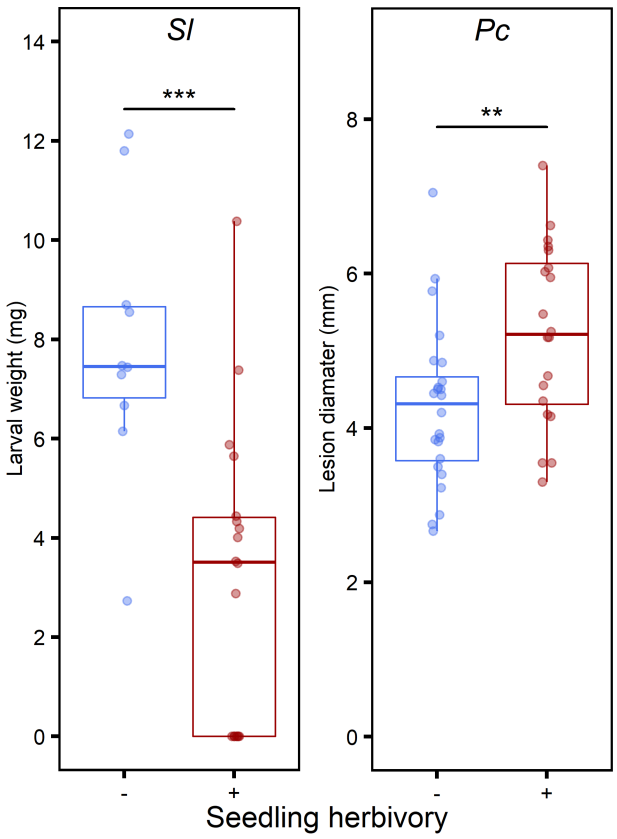

Extended Data Fig. 1 | Herbivore damage at the seedling stage results in long-term IR against herbivory and long-term IS against necrotrophic pathogen infection. Effect of feeding damage by *Spodoptera littoralis* (*Sl*) larvae at the 2-week-old seedling stage on the resistance of 5-week-old Arabidopsis (Col-0) against herbivory by *Sl* larvae (left panel) and disease by necrotrophic *Plectosphaerella cucumerina* (*Pc*; right panel). Data points represent weights of individual *Sl* larvae after feeding on individual plants (n=10-18) or average per plant lesion diameters by *Pc* (n=18-21). Asterisks indicate statistically significant differences between seedling treatments (Mann-Whitney test for *Sl* or two sample t-test for *Pc*; ** $p < 0.01$, *** $p < 0.001$). For more details about experimental design, see legend for Fig. 1.

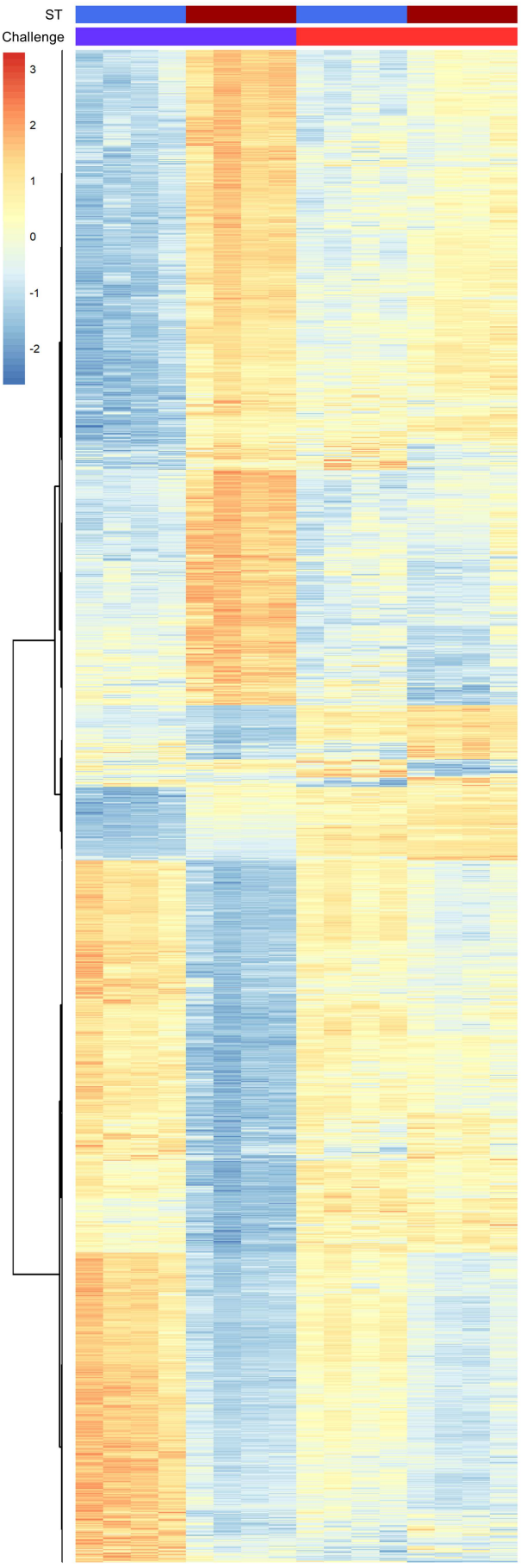

Extended Data Fig. 2 | Selection of genes showing altered JA responsiveness to JA challenge in 5-week-old plants as a consequence of JA seedling treatment. Expression profiles of 2,409 genes with a statistically significant interaction between seedling treatment (ST) and challenge treatment (*p.adj* < 0.01). Replicate samples (*n*=4) for mRNA-seq analysis were collected from 5-week-old plants at 4 hrs after challenge with water (W) or 0.1 mM JA. Plants had been pre-treated with water or 1 mM JA at the seedling stage (2-week-old). Blue and red columns above the heatmap indicate water and JA treatments, respectively. Heatmap-projected values represent per gene z-scores of transformed read counts from all biological replicates.

a

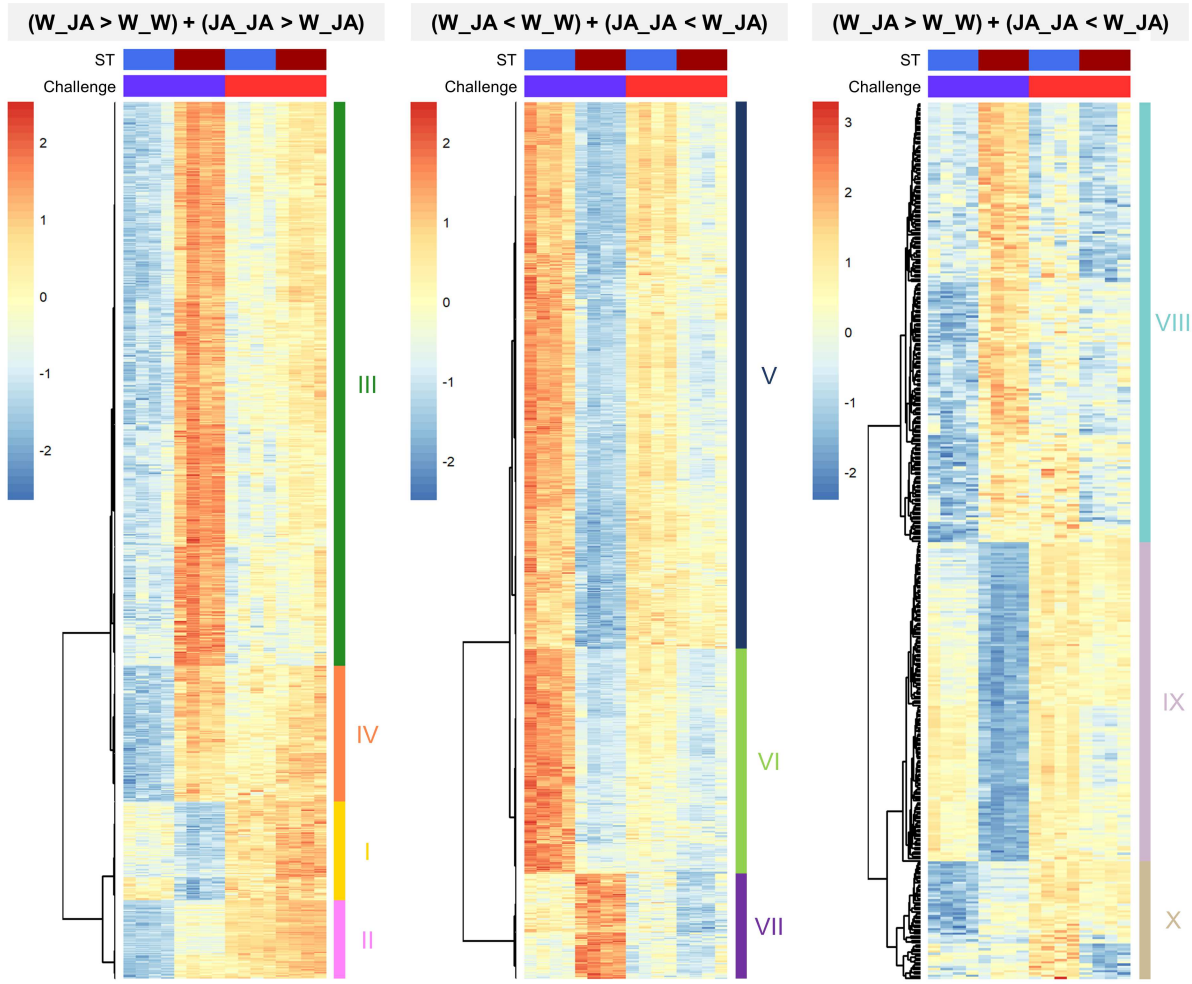

b

Cluster	GO term	GO name	Fold enrichment
II	GO:0009694	jasmonic acid metabolic process	9.60
II	GO:0019760	glucosinolate metabolic process	8.97
II	GO:0009753	response to jasmonic acid	7.68
II	GO:0009611	response to wounding	5.50
IV	GO:0019761	glucosinolate biosynthetic process	7.99

Cluster	GO term	GO name	Fold enrichment
V	GO:0052542	defense response by callose deposition	4.89
V	GO:0009863	salicylic acid mediated signaling pathway	4.27
V	GO:0009627	systemic acquired resistance	3.96
VI	GO:0050832	defense response to fungus	5.11
VI	GO:0009626	plant-type hypersensitive response	4.98
VI	GO:0042742	defense response to bacterium	3.04

Cluster	GO term	GO name	Fold enrichment
IX	GO:0009693	ethylene biosynthetic process	5.58
IX	GO:0009873	ethylene-activated signaling pathway	5.33
IX	GO:0009620	response to fungus	4.58
IX	GO:0009867	jasmonic acid mediated signaling pathway	3.98
IX	GO:0010200	response to chitin	3.63
IX	GO:0009863	salicylic acid mediated signaling pathway	3.28

Extended Data Fig. 3 | Selection of genes with expression profiles and predicted functions that correlate with long-term JA-IR against herbivory (left) and long-term JA-IS against biotrophic (middle) and necrotrophic (right) pathogens. a, Gene expression profiles were selected from the 2,409 genes with a statistically significant interaction between seedling and challenge treatment (*p.adj* < 0.01), using the criteria

displayed above the heatmaps (letters before and after the underscore indicate seedling treatment and challenge, respectively), resulting in 832 (left), 904 (middle) and 395 (right) genes. Replicate samples (*n*=4) for mRNA-seq analysis were collected from 5-week-old plants at 4 hrs after challenge with water (W) or 0.1 mM JA. Plants had been pre-treated with water or 1 mM JA at the seedling stage (2-week-old). Blue and red columns above the heatmaps indicate water and JA treatments, respectively, of seedlings (ST) and 5-week-old plants (Challenge). Heatmap-projected values represent per gene z-scores of transformed read counts from all biological replicates. Numbered boxes next to heatmaps indicate 10 distinct gene expression clusters. **b**, Selection of defence-related Gene Ontology (GO) terms enriched (*p.adj* < 0.05) within the 10 gene clusters shown in (**a**). For complete lists of enriched GO terms, see Supplementary Data 3, 7 and 11.

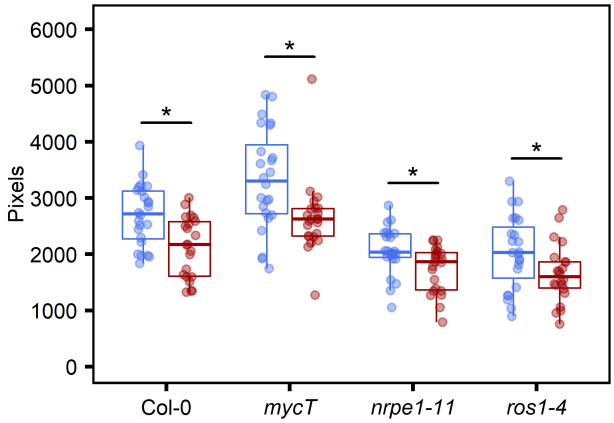

Extended Data Fig. 4 | JA seedling treatment reduces plant growth independently of MYC2/3/4 TFs and RdDM- and ROS1-dependent regulation of DNA methylation. Hyperspectral imaging quantified rosette surface areas of 5-week-old plants (*n*=22-24) pre-treated with water (blue) or 1 mM JA (red) at the seedling stage (2-weeks-old). Asterisks indicate statistically significant within genotype differences between treatments (Wilcoxon rank sum test, * $p < 0.05$).

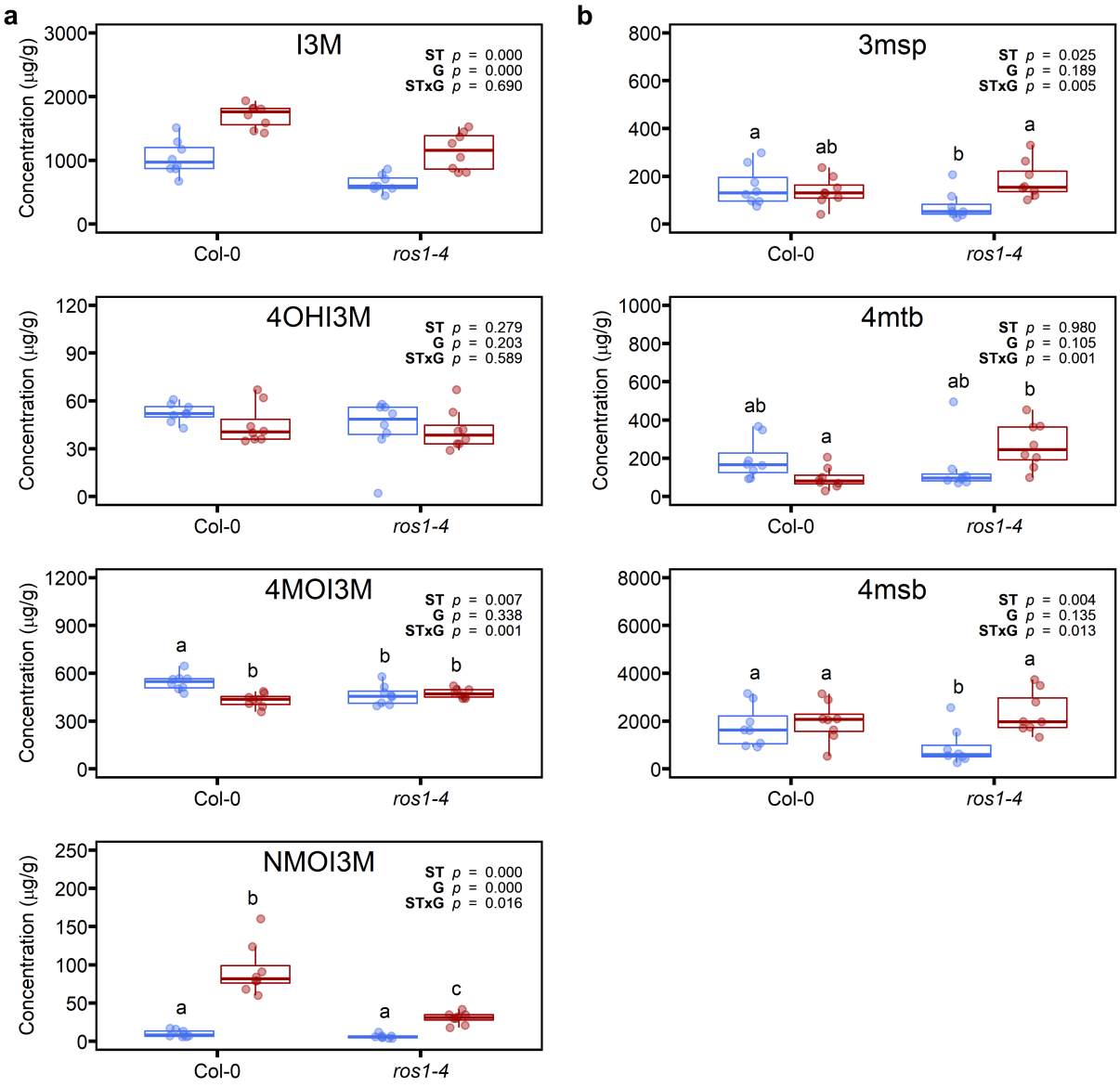

Extended Data Fig. 5 | JA seedling treatment induces long-lasting changes in glucosinolate content that are dependent on the DNA demethylase ROS1. Long-term effects of water (blue) and 1 mM JA (red) treatments of 2-week-old seedlings on the concentrations (µg/g dry mass) of all glucosinolates detected in the leaf tissue of 5-week-old WT (Col-0) and *ros1-4* plants (*n*=8). **a**, Indole glucosinolates. **b**, Aliphatic glucosinolates. If the seedling treatment (ST) x Genotype (G) interaction term was significant (Two-way ANOVA, $p < 0.05$), a Tukey post-doc test was conducted with different letters indicating significant differences between means ($p < 0.05$). I3M: glucobrassicin, 4OHI3M: 4-hydroxyglucobrassicin, 4MOI3M: 4-methoxyglucobrassicin, NMOI3M: neoglucobrassicin, 3msp: glucoiberin, 4mtb: glucoerucin, 4msb: glucoraphanin.

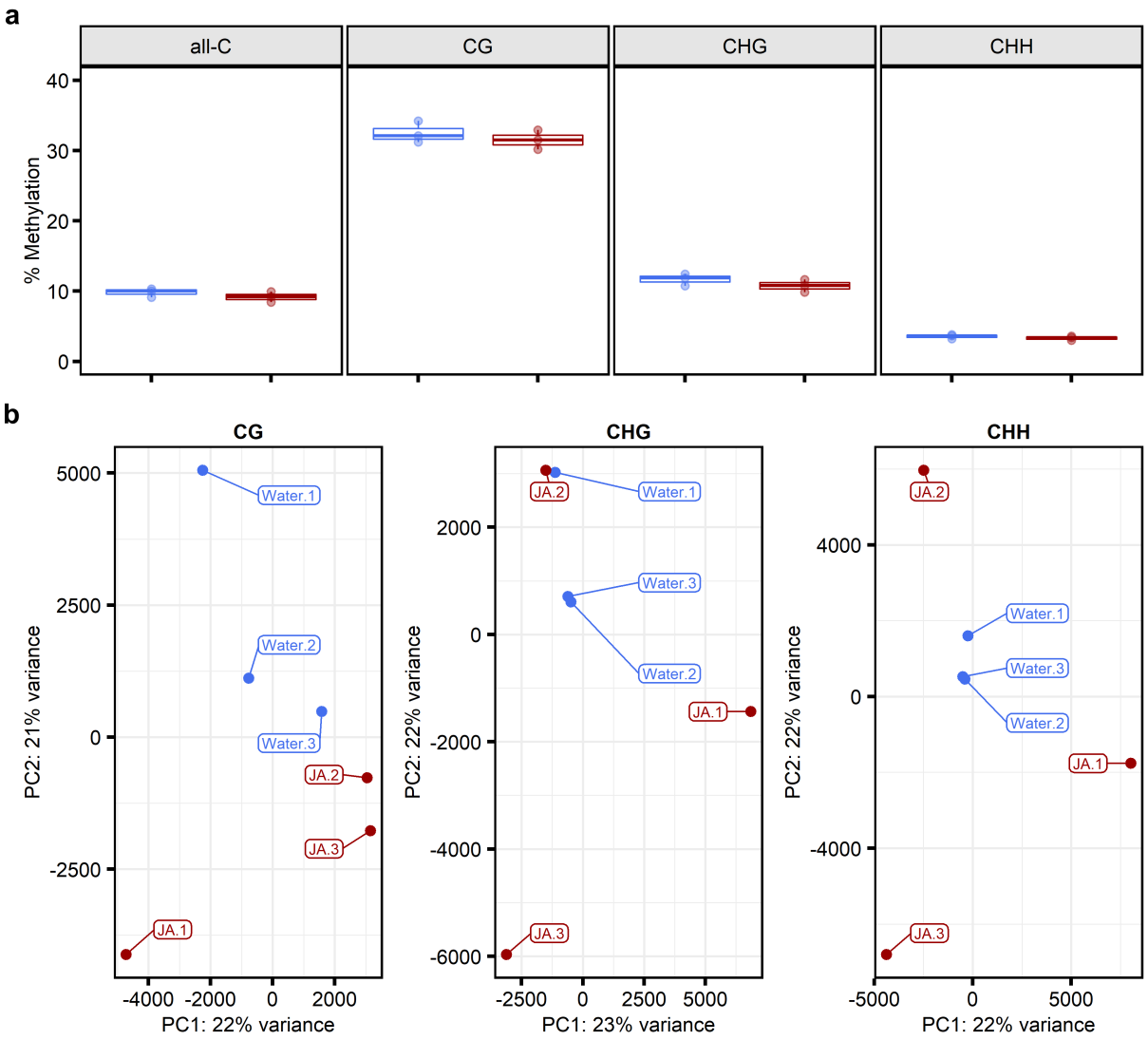

1174 **Extended Data Fig. 6 | Long-term impacts of JA seedling treatment on global DNA**
1175 **methylation levels and patterning. a**, Long-lasting effects of JA on global weighted
1176 cytosine (C) methylation levels at all-C, CG, CHG and CHH contexts (H indicates any
1177 nucleotide other than G). Data points indicate biologically replicated samples (*n*=3) from 5-
1178 week-old plants that had been pre-treated with water (blue) or 1 mM JA (red) at the seedling
1179 stage (2-weeks-old). No statistically significant differences between seedling treatments
1180 were detected (two-sample t-tests, $p > 0.05$). **b**, PCA plots of global methylation at CG, CHG
1181 or CHH contexts.

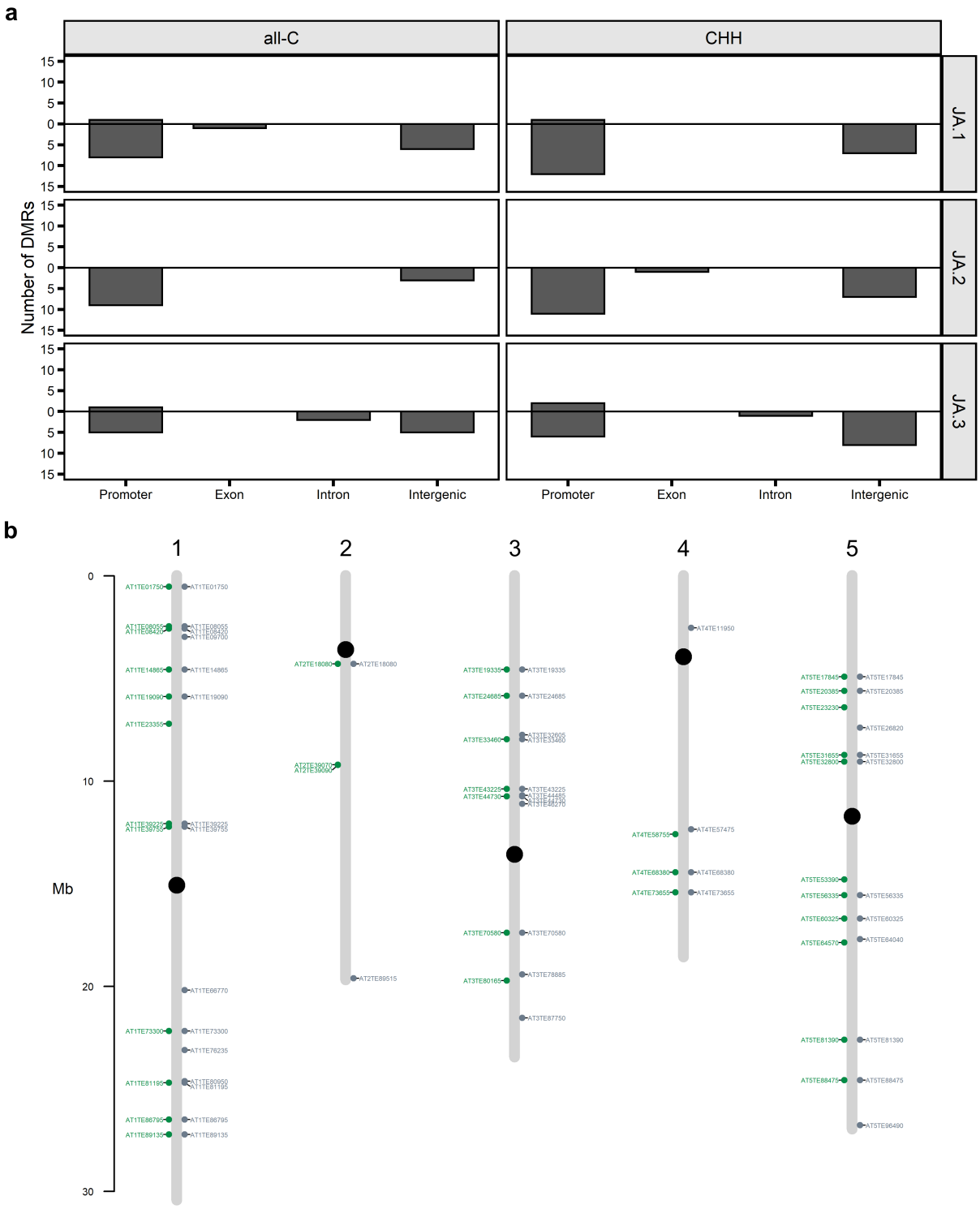

1182 **Extended Data Fig. 7 | Differentially methylated regions in *ATREP2* transposable**
1183 **elements are predominantly hypomethylated and spread across the genome. a**,
1184 Numbers and genomic contexts of differentially methylated regions (DMRs) overlapping with
1185 *ATREP2* transposable elements (TEs). For details about DMR selection, see legend to Fig.
1186 5c. Frequencies of hyper- and hypo-methylated DMRs are indicated by the bars above and

below the x-axis, respectively. **b**, Distribution across the 5 Arabidopsis chromosomes of DMRs overlapping with *ATREP2* TEs. Black dots and grey bars indicate centromeres and chromosomes, respectively. *ATREP2* TEs labelled in green and grey overlapped with DMRs at all-C or CHH sequence contexts, respectively. Shown are all *ATREP2* TEs which overlapped with at least one DMR from one 1JA_vs_3W comparison.

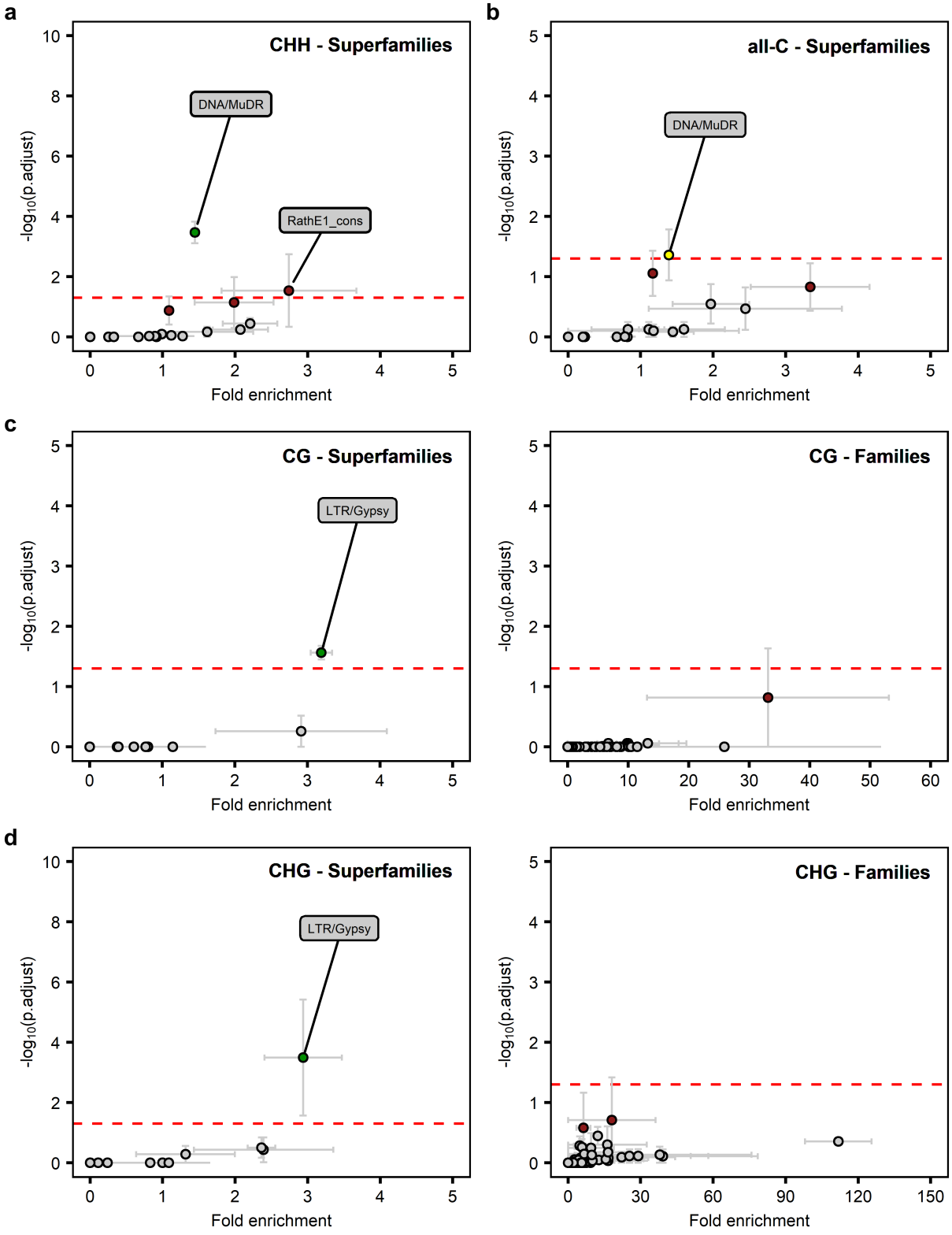

Extended Data Fig. 8 | Transposable element (super)families enriched with JA-induced differentially methylated regions. Shown are transposable element (TE) (super)families enriched with JA-induced differentially methylated regions (DMRs) at CHH (**a**), all-C (**b**), CG (**c**) and CHG (**d**) sequence contexts. For details about DMR selection, see

legend to Fig. 5. Enriched TE families for CHH and all-C contexts are displayed in Fig. 5d,e. Graphs plot statistical significance against the corresponding fold-enrichment, represented by mean $-\log_{10}(p.adj)$ values (± SEM) and mean fold enrichment values (± SEM), respectively. Enrichment is expressed relative to the background of all genome annotated TEs (TAIR v10). Labelled data points indicate TE (super)families with a mean $-\log_{10}(p.adj) > -\log_{10}(0.05)$ (red dashed line). Brightly coloured data points indicate TE (super)families that were significantly ($p.adj \leq 0.05$) overrepresented in 1 (red), 2 (yellow) or 3 (green) comparisons, respectively.

SUPPLEMENTARY TABLES

Supplementary Table 1 | Ingredients of the *Spodoptera littoralis* diet.

Supplementary Table 2 | RT-qPCR primers.

SUPPLEMENTARY DATA

Supplementary Data 1 | mRNA-seq read counts for genes displaying an altered response to JA challenge as a result of prior JA seedling treatment.

Supplementary Data 2 | mRNA-seq read counts for the 832 genes selected by the criteria (W_JA > W_W) and (JA_JA > W_JA).

Supplementary Data 3 | GO terms that are statistically enriched in gene clusters I-IV of Extended Data Fig. 3a.

Supplementary Data 4 | mRNA-seq read counts for the 203 genes associated with long-term JA-IR against *Sl*.

Supplementary Data 5 | GO terms that are statistically enriched among the 203 genes associated with long-term JA-IR against *Sl*.

Supplementary Data 6 | mRNA-seq read counts for the 904 genes selected by the criteria (W_JA < W_W) and (JA_JA < W_JA).

Supplementary Data 7 | GO terms that are statistically enriched in gene clusters V-VII of Extended Data Fig. 3a.

Supplementary Data 8 | mRNA-seq read counts for the 796 genes associated with long-term JA-IS to *Pst*.

Supplementary Data 9 | GO terms that are statistically enriched among the 796 genes associated with long-term JA-IS to *Pst*.

Supplementary Data 10 | mRNA-seq read counts for the 395 genes selected by the criteria (W_JA > W_W) and (JA_JA < W_JA).

Supplementary Data 11 | GO terms that are statistically enriched in gene clusters VIII-X of Extended Data Fig. 3a.

Supplementary Data 12 | mRNA-seq read counts for the 144 genes associated with long-term JA-IS to *Pc*.

Supplementary Data 13 | GO terms that are statistically enriched among the 144 genes associated with long-term JA-IS to *Pc*.

Supplementary Data 14 | Transcription factor DNA binding motifs that are overrepresented within promoters of the 203 genes associated with long-term JA-IR to *Sl*.

Supplementary Data 15 | DMR locations and statistics.

Supplementary Data 16 | DMR summary statistics.

Supplementary Data 17 | Consensus DMRs**.**

Supplementary Data 18 | Raw read data and alignment statistics of the mRNA sequencing analysis.

Supplementary Data 19 | Raw read data and alignment statistics of the whole genome bisulfite sequencing analysis.

Supplementary Files

This is a list of supplementary files associated with this preprint. Click to download.

- rs148432suppTables.pdf
- suppdata01.xlsx
- suppdata02.xlsx
- suppdata03.xlsx
- suppdata04.xlsx
- suppdata05.xlsx
- suppdata06.xlsx
- suppdata07.xlsx
- suppdata08.xlsx
- suppdata09.xlsx
- suppdata10.xlsx
- suppdata11.xlsx
- suppdata12.xlsx
- suppdata13.xlsx
- suppdata14.xlsx
- suppdata15.xlsx
- suppdata16.xlsx
- suppdata17.xls
- suppdata18.xlsx
- suppdata19.xlsx